Fragmentation Functions and Global QCD Fits

Lecture 3: Phenomenology of Fragmentation Functions

Outline

1. Recap of Lectures 1-2
   factorisation, evolution, parametrisation
   modern sets of Fragmentation Functions
2. Fits to SIA data only: the NNFF1.0 analysis (pions and kaons)
   data set; observables
   fit settings; fit quality
   dependence upon the perturbative order/data set/kinematic cuts
   high-energy resummed FFs
3. Global fits: the DEHSS analyses (pions and kaons)
   fit settings; data sets; fit quality
   data/theory comparison: SIDIS multiplicitites and pp data
   impact of various flavour schemes
4. Interlude: the helicity structure of the proton
   polarised PDFs and the spin of the proton
   the NNPDF analyses: achievements and open issues
5. A simultaneous determination of PDFs/FFs
   the JAM analysis
   a new insight into the polarised strangeness conundrum

A selection of some of the most recent results available in the literature

3.1 Recap of Lectures 1-2

Recap of Lecture 1

Fragmentation functions encode the information on how partons produced in a hard-scattering process are turned into an observed colorless hadronic bound final-state

$$d\sigma^h(x,Q^2) = \sum_{i=-n_f}^{n_f} \int_x^1 dz\, d\sigma^i\left(\frac{x}{z}, \frac{Q^2}{\mu^2}, \frac{m_i^2}{Q^2}, \alpha_s(\mu^2)\right) D_i^h(z,\mu^2)$$

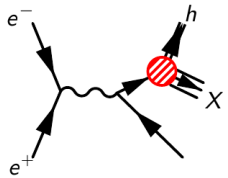

$e^+ + e^- \to h + X$

single-inclusive annihilation (SIA)

$$\frac{d\sigma^h}{dz} = F_T^h(z,Q^2) + F_L^h(z,Q^2) = F_2^h(x,Q^2)$$

$$F_{k=T,L,2}^h = \frac{4\pi\alpha_{\rm em}^2}{Q^2}\langle e^2\rangle \left\{ D_\Sigma^h \otimes \mathcal{C}_{k,q}^{\rm S} + n_f D_g^h \otimes \mathcal{C}_{k,g}^{\rm S} + D_{\rm NS}^h \otimes \mathcal{C}_{k,q}^{\rm NS} \right\}$$

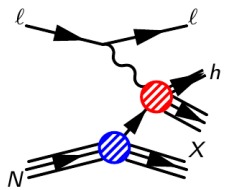

SIDIS

$\ell + N \to \ell' + h + X$

semi-inclusive deep-inelastic scattering (SIDIS)

$$\frac{d\sigma^h}{dxdydz} = \frac{2\pi\alpha_{em}^2}{Q^2}\left[\frac{1+(1-y)^2}{y} 2F_1^h + \frac{2(1-y)}{y} F_L^h\right]$$

$$2F_1^h = e_q^2 \left\{ q \otimes D_q^h + \frac{\alpha_s}{2\pi}\left[q \otimes C_{qq}^1 \otimes D_q^h + q \otimes C_{gq}^1 \otimes D_g^h + g \otimes C_{qg}^1 \otimes D_q^h \right] \right\}$$

$$F_L^h = \frac{\alpha_s}{2\pi} \sum_{q,\bar q} e_q^2 \left[q \otimes C_{qq}^L \otimes D_q^h + q \otimes C_{gq}^L \otimes D_g^h + g \otimes C_{qg}^L \otimes D_q^h \right]$$

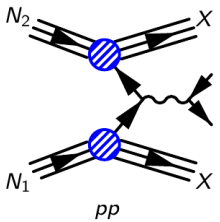

$N_1 + N_2 \to h + X$

high-p_T hadron production in pp collisions (PP)

$$E_h \frac{d^3\sigma}{dp_h^3} = \sum_{a,b,c} f_a \otimes f_b \otimes \hat\sigma_{ab}^c \otimes D_c^h$$

$$= \sum_{i,j,k,l} \int \frac{dx_a}{x_a} \int \frac{dx_b}{x_b} \int \frac{dz}{z^2} f^{i/p_a}(x-a) f^{j/p_b} D^{h/k}(z) \hat\sigma^{ij\to kl} \delta(\hat s + \hat t + \hat u)$$

Recap of Lectures 1-2

1. Factorisation of physical observables

$$\mathcal{O}_I(x,Q^2) = \sum_j C_{Ij}(x,\alpha_s(Q^2)) \otimes f_j(x,Q^2)$$

2. DGLAP evolution of PDFs/FFs

$$Q^2 \frac{\partial}{\partial Q^2} f_i(x,Q^2) = \sum_j P_{ij}(x,\alpha_s(Q^2)) \otimes f_j(x,Q^2)$$

3. Solution of the DGLAP equtions

$$f_i(x,Q^2) = \sum_j \Gamma_{ij}(x,\alpha_s(Q^2),\alpha_s(Q_0^2)) \otimes f_j(x,Q_0^2)$$

4. Separation between the perturbative and nonperturbative parts in any observable

$$\mathcal{O}_I(x,Q^2) = \sum_{jk} C_{Ij}(x,\alpha_s(Q^2)) \otimes \Gamma_{jk}(x,\alpha_s(Q^2),\alpha_s(Q_0^2)) \otimes f_k(x,Q_0^2)$$

5. (pre-)compute the perturbative hard kernel

$$K_{Ij}(x,\alpha_s(Q^2),\alpha_s(Q_0^2)) = \sum_k C_{Ik}(x,\alpha_s(Q^2)) \otimes \Gamma_{kj}(x,\alpha_s(Q^2),\alpha_s(Q_0^2))$$

6. Parametrise the nonperturbative PDFs/FFs $f_k(x,Q_0^2)$ at the initial scale Q_0^2

Modern determinations of Fragmentation Functions

	DHESS	HKNS	JAM	NNFF1.0
SIA	☑	☑	☑	☑
SIDIS	☑	☒	☒	☒
PP	☑	☒	☒	☑
statistical treatment	Iterative Hessian 68% - 90%	Hessian $\Delta\chi^2 = 15.94$	Monte Carlo	Monte Carlo
parametrisation	standard	standard	standard	neural network
HF scheme	ZM-VFN	ZM-VFN	ZM-VFN	ZM-VFN
hadron species	$\pi^\pm$, $K^\pm$, $p/\bar{p}$, $h^\pm$	$\pi^\pm$, $K^\pm$, $p/\bar{p}$	$\pi^\pm$, $K^\pm$	$\pi^\pm$, $K^\pm$, $p/\bar{p}$
latest update	PRD 91 (2015) 014035 PRD 95 (2017) 094019	PTEP 2016 (2016) 113B04	PRD 94 (2016) 114004	in preparation

+ some others (including analyses for specific hadrons)

BKK95 [ZPB 65 (1995) 471]	$\pi^\pm, K^\pm$
BKK96 [PRD 53 (1996) 3553]	K^0
DSV97 [PRD 57 (1998) 5811]	Λ^0
BFGW00 [EPJ C19 (2001) 89]	$h^\pm$

AESS11 [PRD 83 (2011) 034002]	η
SKMNA13 [PRD 88 (2013) 054019]	$\pi^\pm, K^\pm$
LSS15 [PRD 96 (2016) 074026]	SIDIS only

some of these determinations are publicly available at

`http://lapth.cnrs.fr/ffgenerator/`

Focus on π and K which constitute the largest fraction in measured yields

3.2 Fits to SIA data only: the NNFF1.0 analysis

The dataset

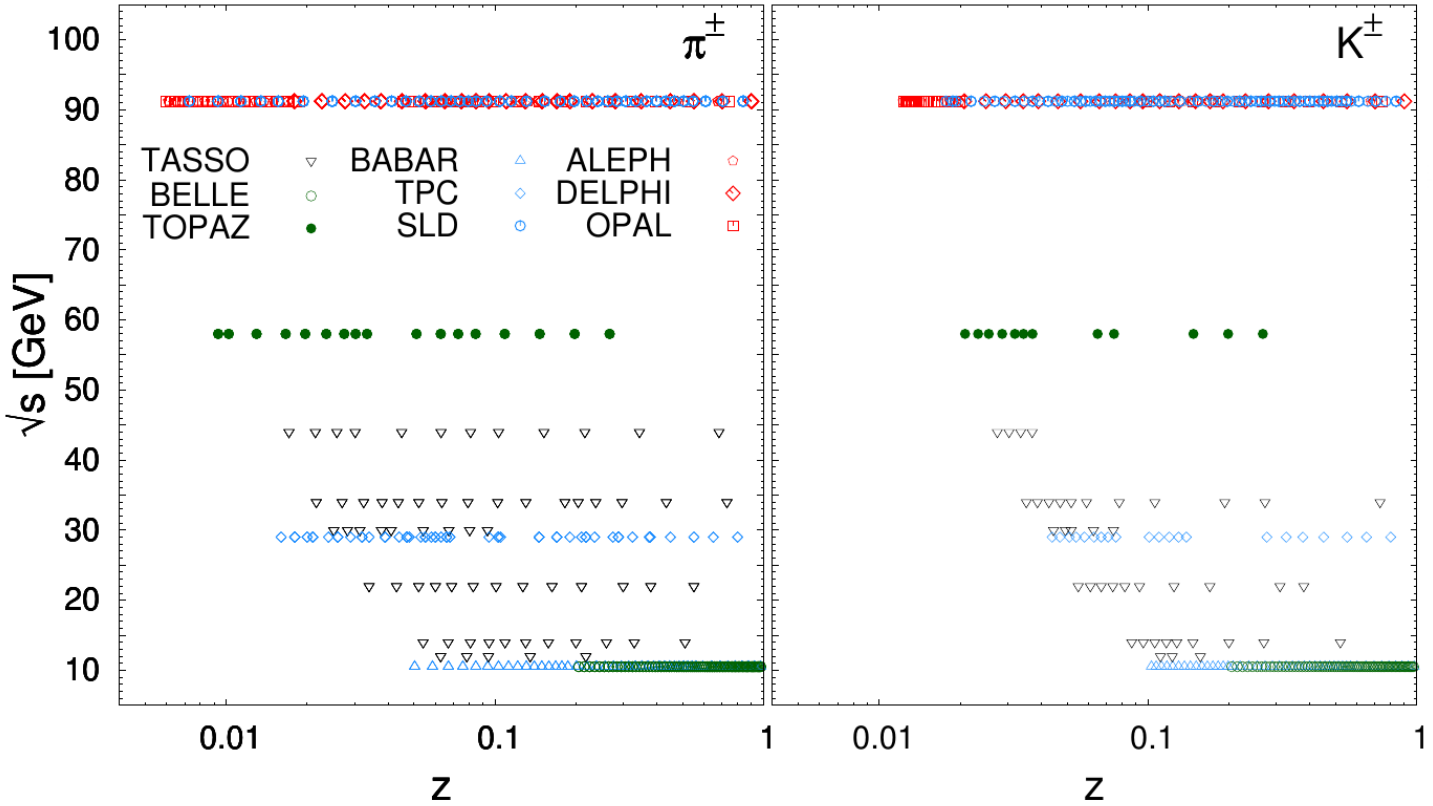

CERN-LEP: ALEPH [ZP C66 (1995) 353] DELPHI [EPJ C18 (2000) 203] OPAL [ZP C63 (1994) 181]

KEK: BELLE ($n_f = 4$) [PRL 111 (2013) 062002] TOPAZ [PL B345 (1995) 335]

DESY-PETRA: TASSO [PL B94 (1980) 444, ZP C17 (1983) 5, ZP C42 (1989) 189]

SLAC: BABAR ($n_f = 4$) [PR D88 (2013) 032011] SLD [PR D58 (1999) 052001] TPC [PRL 61 (1988) 1263]

$$\frac{d\sigma^h}{dz} = \frac{4\pi\alpha^2(Q^2)}{Q^2} F_2^h(z,Q^2) \quad h = \pi^+ + \pi^-,\, K^+ + K^-; \quad \text{possibly normalised to } \sigma_{\rm tot}$$

From observables to fragmentation functions

$$\boxed{\mathcal{F}_2^h = \langle e^2 \rangle \left\{ C_{2,q}^{\rm S} \otimes D_\Sigma^h + n_f C_{2,g}^{\rm S} \otimes D_g^h + C_{2,q}^{\rm NS} \otimes D_{\rm NS}^h \right\}}$$

$$\langle e^2 \rangle = \frac{1}{n_f} \sum_{q=1}^{n_f} \hat{e}_q^2 \qquad D_\Sigma^h = \sum_{q=1}^{n_f} D_{q^+}^h \qquad D_{\rm NS}^h = \sum_{q=1}^{n_f} \left(\frac{\hat{e}_q^2}{\langle e^2 \rangle} - 1 \right) D_{q^+}^h \qquad D_{q^+}^h = D_q^h + D_{\bar{q}}^h$$

Coefficient functions and splitting functions known up to NNLO

[NPB 751 (2006) 18; NPB 749 (2006) 1; PLB 638 (2006) 61; NPB 845 (2012) 133]

$$\begin{aligned} F_2^{h,n_f=5} =& \frac{1}{5} \left[\left(2\hat{e}_u^2 + 3\hat{e}_d^2\right) C_{2,q}^{\rm S} + 3 \left(\hat{e}_u^2 - \hat{e}_d^2\right) C_{2,q}^{\rm NS} \right] \otimes \left(D_{u^+}^h + D_{c^+}^h \right) \\ &+ \frac{1}{5} \left[\left(2\hat{e}_u^2 + 3\hat{e}_d^2\right) C_{2,q}^{\rm S} - 2 \left(\hat{e}_u^2 - \hat{e}_d^2\right) C_{2,q}^{\rm NS} \right] \otimes \left(D_{d^+}^h + D_{s^+}^h + D_{b^+}^h \right) \\ &+ \left(2\hat{e}_u^2 + 3\hat{e}_d^2\right) C_{2,g}^{\rm S} \otimes D_g^h \end{aligned}$$

No sensitivity to individual quark and antiquark FFs

Limited sensitivity to flavour separation via the variation of $\hat{e}_q$ with Q^2

$\hat{e}_u^2/\hat{e}_d^2(Q^2 = 10\,{\rm GeV}) \sim 4 \Rightarrow D_{u^+}^h,\ D_{d^+}^h + D_{s^+}^h$; $\quad \hat{e}_u^2/\hat{e}_d^2(Q^2 = M_Z) \sim 0.8 \Rightarrow D_\Sigma^h$

Flavor separation between uds and c, b quarks achieved thanks to tagged data

Direct sensitivity to D_g^h only beyond LO, as $C_{2,g}^{\rm S}$ is $\mathcal{O}(\alpha_s^2)$, and tenous

Indirect sensitivity to D_g^h via scale violations in the time-like DGLAP evolution

Fit settings

Physical parameters: consistent with the `NNPDF3.1` PDF set [arXiv:1706.00428]

$$\alpha_s(M_Z) = 0.118,\ \alpha(M_Z) = 1/127,\ m_c = 1.51 \text{ GeV},\ m_b = 4.92 \text{ GeV}$$

Solution of DGLAP equations: numerical solution in z-space as implemented in `APFEL`

extensive benchmark performed up to NNLO [JHEP 1503 (2015) 046]

Parametrisation: each FF is parametrised with a feed-forward neural network (2-5-3-1)

$$D_i^h(Q_0, z) = \text{NN}(x) - \text{NN}(1),\ \ Q_0 = 5 \text{ GeV}$$

PIONS

$$h = \pi^+ + \pi^-,\ i = u^+, s^+, c^+, b^+, g$$

$D_{u^+}^{\pi^\pm} = D_{d^+}^{\pi^\pm}$ (isospin symmetry)

KAONS

$$h = K^+ + K^-,\ i = u^+, d^+ + s^+, c^+, b^+, g$$

no further theoretical assumptions

we assume charge conjugation, from which $D_{q^+}^{\pi^+} = D_{q^+}^{\pi^-}$

initial scale above m_b, but below the lowest c.m. energy of the data, avoid threshold crossing

Heavy flavours: heavy-quark FFs are parametrised independently at the initial scale Q_0

Kinematic cuts: $z \to 0$: contributions $\propto \ln z$; $z \to 1$: contributions $\propto \ln(1-z)$

PIONS

$z_{\min} = 0.1$, $z_{\min} = 0.05$ ($\sqrt{s} = M_Z$); $z_{\max} = 0.90$

$z_{\min} = 0.075$, $z_{\min} = 0.01$ ($\sqrt{s} = M_Z$); $z_{\max} = 0.90$

KAONS

$z_{\min} = 0.2$, $z_{\min} = 0.1$ ($\sqrt{s} = M_Z$); $z_{\max} = 0.90$

$z_{\min} = 0.1$, $z_{\min} = 0.05$ ($\sqrt{s} = M_Z$); $z_{\max} = 0.90$

Fit quality: π^+

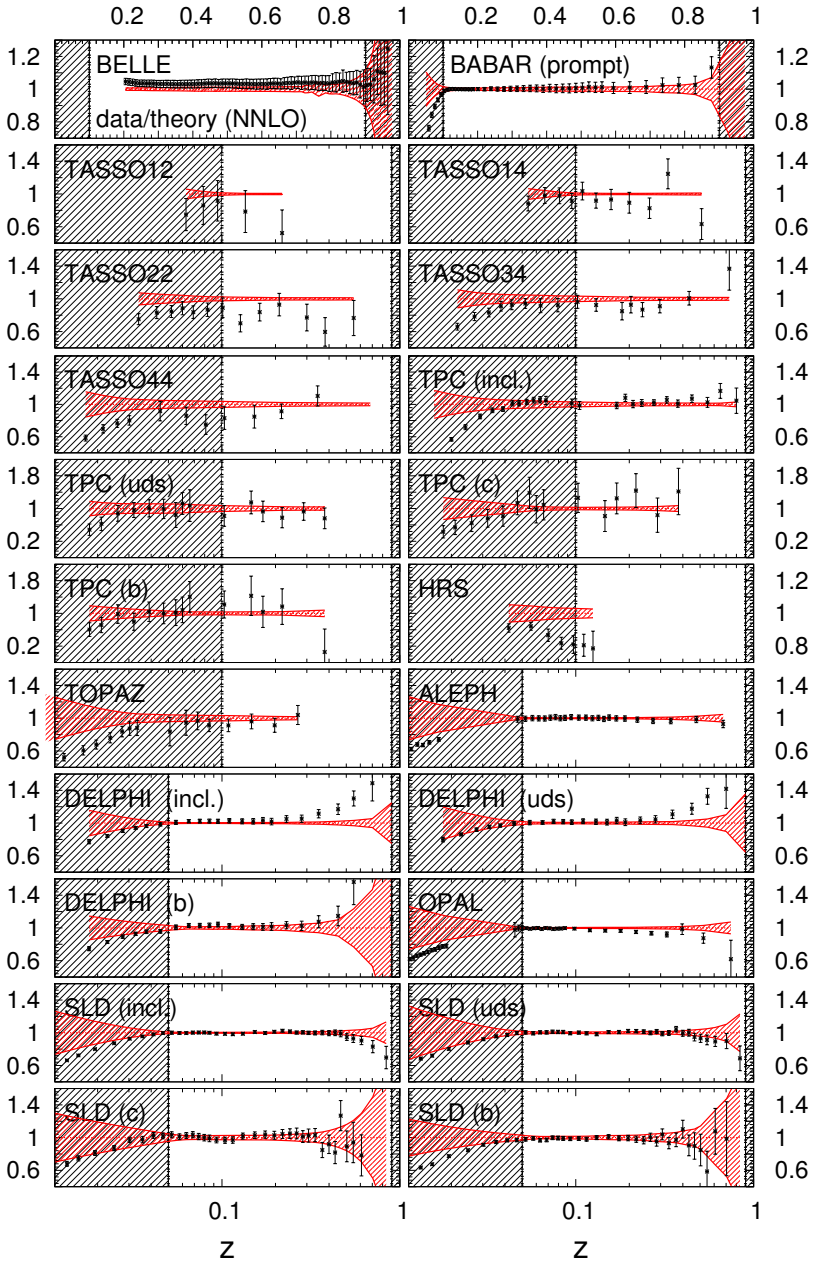

Exp.	$N_{\rm dat}$	NNLO theory $\chi^2/N_{\rm dat}$	remarks
BELLE	70	0.08	lack of correlations
BABAR	37	1.17	☑
TASSO12	2	1.61	small sample
TASSO14	7	1.83	} data fluctuations
TASSO22	7	2.16	
TASSO34	8	1.09	☑
TASSO44	5	1.95	data fluctuations
TPC	12	0.98	☑
TPC-UDS	6	0.45	☑
TPC-C	6	0.50	☑
TPC-B	6	1.41	☑
TOPAZ	4	0.66	☑
ALEPH	22	0.88	☑
DELPHI	16	2.32	tension with OPAL
DELPHI-UDS	16	1.90	tension with OPAL
DELPHI-B	16	1.09	☑
OPAL	22	2.05	tension with DELPHI
SLD	29	1.09	☑
SLD-UDS	29	0.80	☑
SLD-C	29	0.97	☑
SLD-B	29	0.44	☑
TOTAL	378	0.99	☑

Overall good description of the dataset
Signs of tension OPAL vs DELPHI (inclusive)
Anomalously small $\chi^2/N_{\rm dat}$ for BELLE

Fit quality: K^+

Exp.	$N_{\rm dat}$	NNLO theory $\chi^2/N_{\rm dat}$	remarks
BELLE	70	0.19	lack of correlations
BABAR	28	0.77	☑
TASSO14	3	1.30	small sample
TASSO22	2	0.29	small sample
TASSO34	2	0.09	small sample
TPC	7	1.19	☑
ALEPH	13	0.72	☑
DELPHI	11	0.17	☑
DELPHI-UDS	11	1.97	☑
DELPHI-B	11	0.41	☑
OPAL	9	2.10	tension with other M_Z data
SLD	21	0.77	☑
SLD-UDS	21	1.11	☑
SLD-C	20	0.42	☑
SLD-B	21	0.71	☑
TOTAL	250	0.67	☑

Overall good description of the dataset
Excellent BELLE/BABAR consistency
Signs of tension OPAL vs DELPHI (inclusive)
Anomalously small $\chi^2/N_{\rm dat}$ for BELLE
Data description rapidly deteriorates at low z
Prediction uncertainties blow up at low z

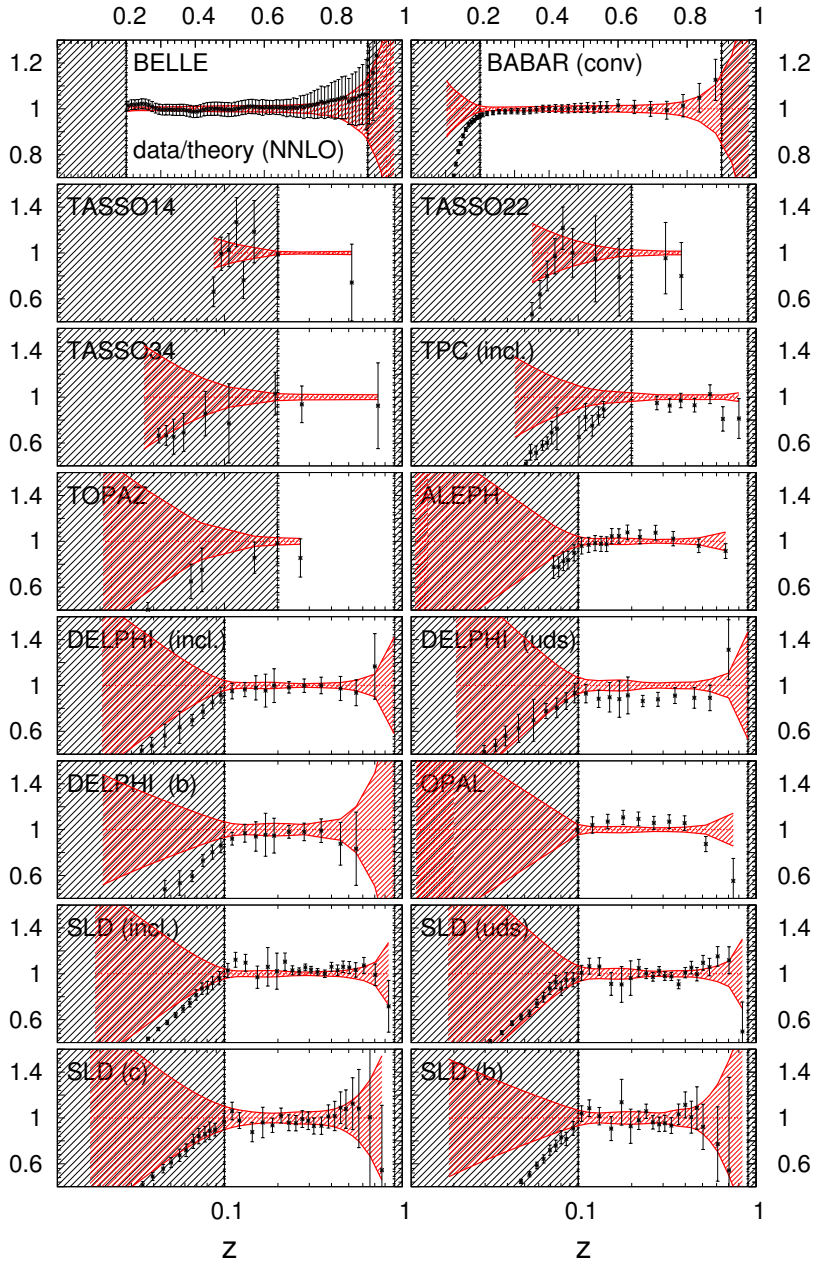

Dependence upon perturbative order: π^+

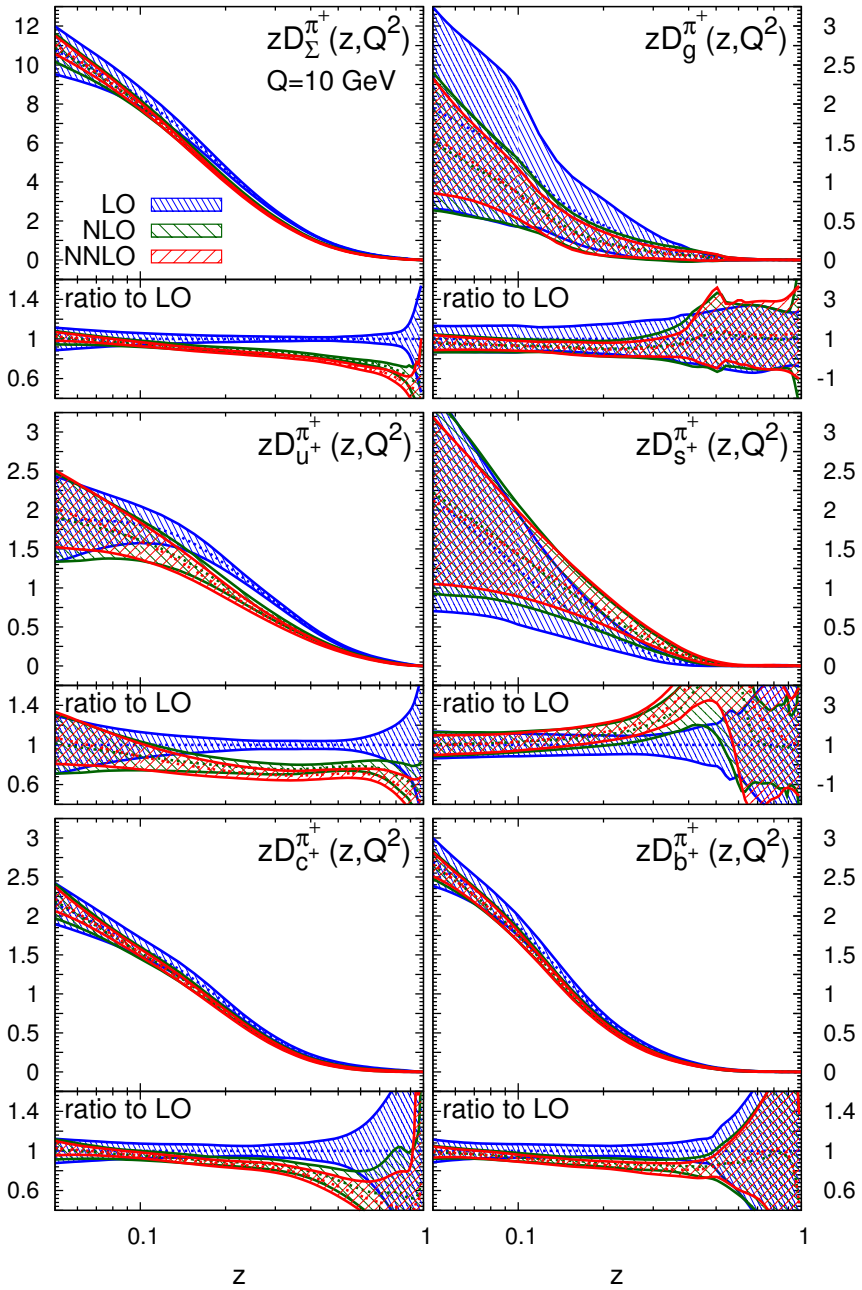

Exp.	$N_{\rm dat}$	LO $\chi^2/N_{\rm dat}$	NLO $\chi^2/N_{\rm dat}$	NNLO $\chi^2/N_{\rm dat}$
BELLE	70	0.67	0.12	0.08
BABAR	37	1.64	1.26	1.17
TASSO12	2	1.19	1.57	1.61
TASSO14	7	1.60	1.81	1.83
TASSO22	7	1.81	2.19	2.16
TASSO34	8	1.26	1.11	1.09
TASSO44	5	2.05	2.00	1.95
TPC	12	0.51	0.69	0.98
TPC-UDS	6	0.79	0.52	0.45
TPC-C	6	0.54	0.51	0.50
TPC-B	6	1.45	1.41	1.41
TOPAZ	4	1.25	0.75	0.66
ALEPH	22	2.25	1.10	0.88
DELPHI	16	1.63	2.17	2.32
DELPHI-UDS	16	1.40	1.75	1.90
DELPHI-B	16	1.45	1.18	1.09
OPAL	22	2.68	2.19	2.05
SLD	29	2.66	1.35	1.09
SLD-UDS	29	1.63	0.98	0.80
SLD-C	29	2.39	1.15	0.97
SLD-B	29	0.45	0.43	0.44
TOTAL	378	1.50	1.05	0.99

Excellent perturbative convergence
FFs almost stable from NLO to NNLO
LO FF uncertainties larger than HO

Dependence upon perturbative order: π^+ [PRD 92 (2015) 114017]

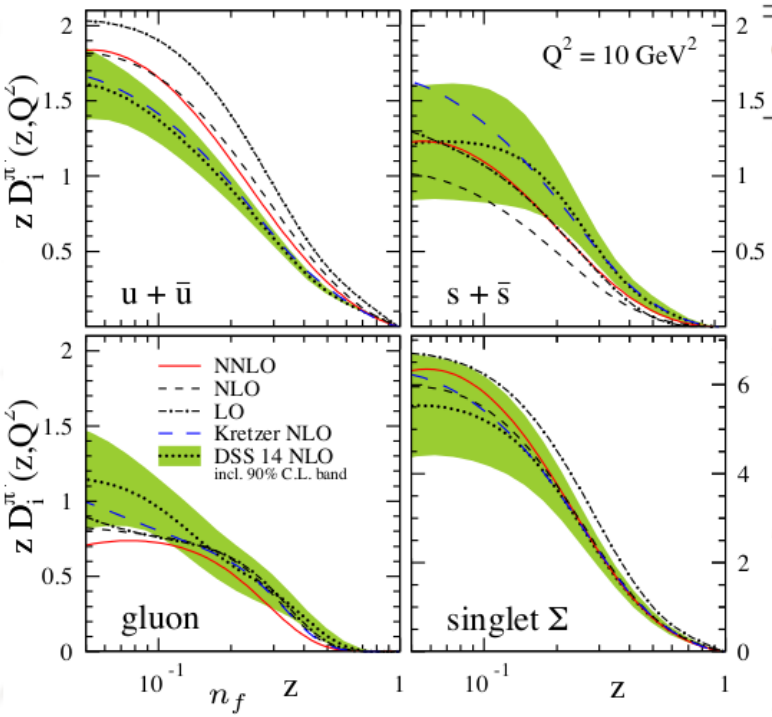

$$D_\Sigma^h = \sum_{i=1}^{n_f} \left(D_{q_i}^h + D_{\bar{q}_i}^h \right)$$

Kretzer FFS (*Phys. Rev. D 62, 054001 (2000)*)

DSS FFS (*Phys. Rev. D 91, 014035 (2015)*)

experiment	data type	# data in fit	χ^2 LO	NLO	NNLO
SLD [40]	incl.	23	15.0	14.8	15.5
	uds tag	14	9.7	18.7	18.8
	c tag	14	10.4	21.0	20.4
	b tag	14	5.9	7.1	8.4
ALEPH [41]	incl.	17	19.2	12.8	12.6
DELPHI [42]	incl.	15	7.4	9.0	9.9
	uds tag	15	8.3	3.8	4.3
	b tag	15	8.5	4.5	4.0
OPAL [43]	incl.	13	8.9	4.9	4.8
TPC [44]	incl.	13	5.3	6.0	6.9
	uds tag	6	1.9	2.1	1.7
	c tag	6	4.0	4.5	4.1
	b tag	6	8.6	8.8	8.6
BABAR [10]	incl.	41	108.7	54.3	37.1
BELLE [9]	incl.	76	11.8	10.9	11.0
NORM. SHIFTS			7.4	6.8	7.1
TOTAL:		288	241.0	190.0	175.2

Slide: courtesy of D. P. Anderle

Dependence upon perturbative order: K^+

Exp.	$N_{\rm dat}$	LO $\chi^2/N_{\rm dat}$	NLO $\chi^2/N_{\rm dat}$	NNLO $\chi^2/N_{\rm dat}$
BELLE	70	0.37	0.34	0.19
BABAR	28	1.02	0.96	0.77
TASSO14	3	1.23	1.24	1.30
TASSO22	2	0.29	0.32	0.29
TASSO34	2	0.02	0.03	0.09
TPC	7	0.41	0.49	1.19
ALEPH	13	0.66	0.71	0.72
DELPHI	11	0.17	0.16	0.17
DELPHI-UDS	11	2.01	1.94	1.97
DELPHI-B	11	0.51	0.44	0.41
OPAL	9	2.02	2.08	2.10
SLD	21	0.81	0.80	0.77
SLD-UDS	21	1.16	1.19	1.11
SLD-C	20	0.49	0.46	0.42
SLD-B	21	0.71	0.68	0.71
TOTAL	250	0.73	0.72	0.67

Excellent perturbative convergence
FFs almost stable from NLO to NNLO
LO FF uncertainties larger than HO

i	$N^{i+1}LO/N^iLO$	D_g	D_Σ	D_{c+}	D_{b+}
0	NLO/LO [%]	95-300	70-80	65-80	70-85
1	NNLO/NLO [%]	70-130	90-100	90-110	95-115

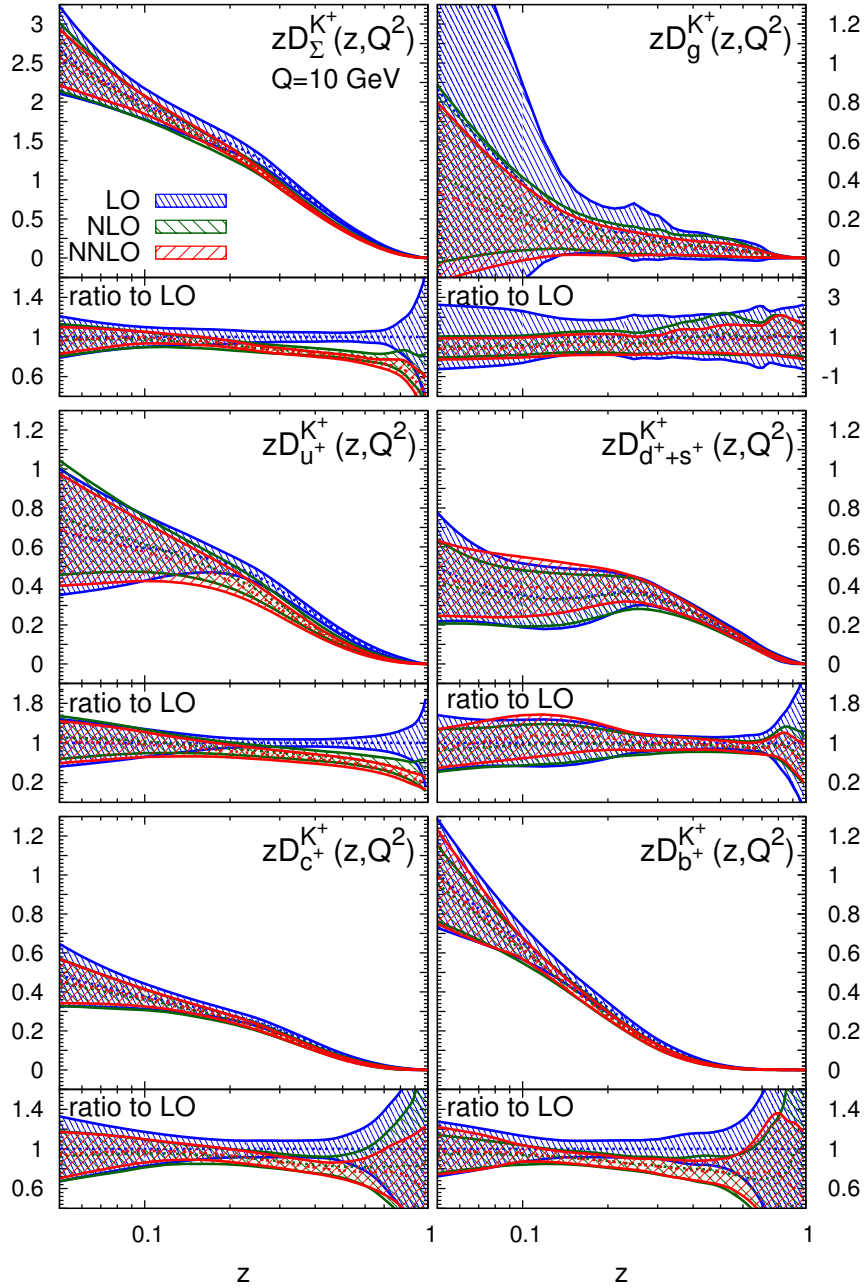

Dependence upon the dataset: π^+

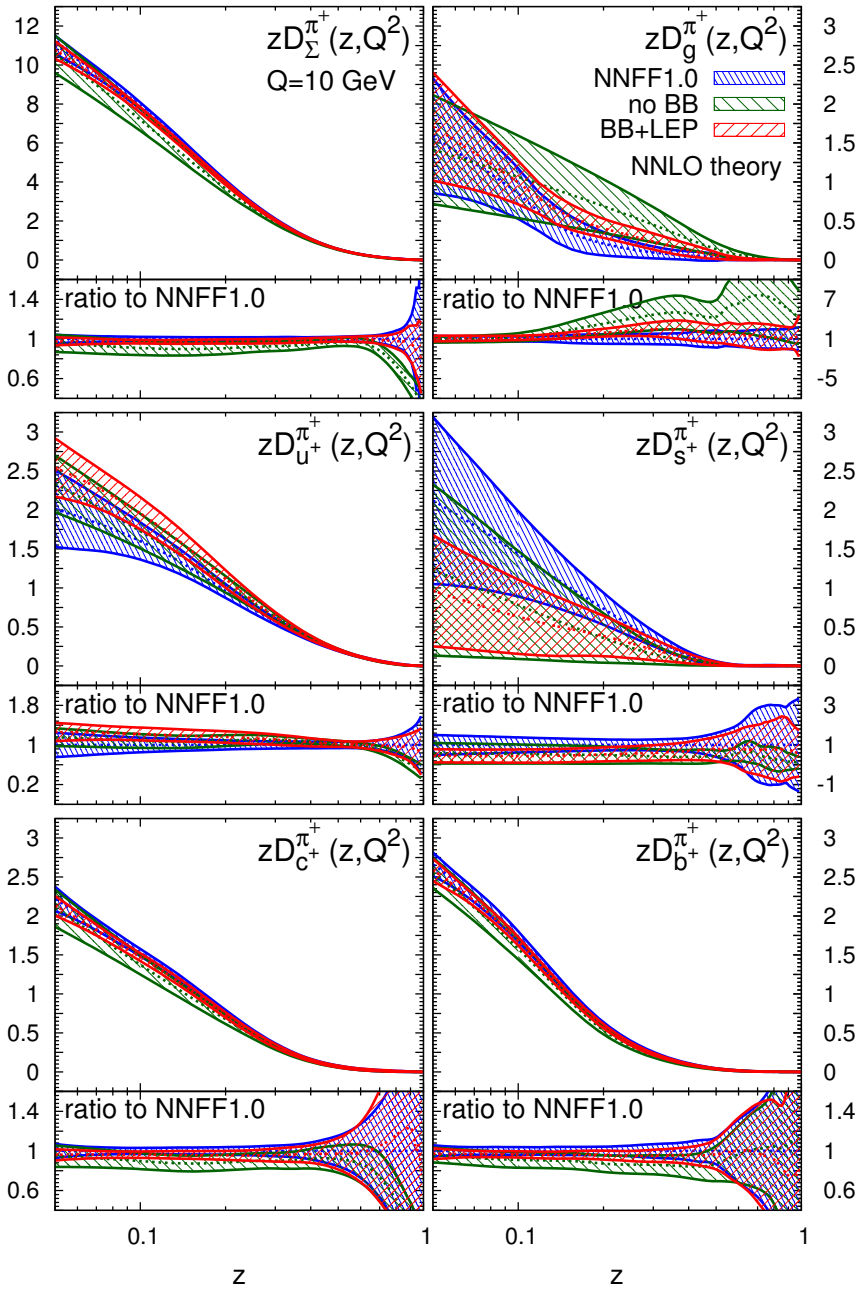

NNLO theory Exp.	$N_{\rm dat}$	NNFF1.0 $\chi^2/N_{\rm dat}$	no BB $\chi^2/N_{\rm dat}$	BB+LEP $\chi^2/N_{\rm dat}$
BELLE	70	0.08	(5.95)	0.08
BABAR	37	1.17	(82.2)	1.22
TASSO12	2	1.61	0.84	(1.61)
TASSO14	7	1.83	1.77	(1.85)
TASSO22	7	2.16	1.55	(2.48)
TASSO34	8	1.09	1.35	(1.55)
TASSO44	5	1.95	2.22	(2.60)
TPC	12	0.98	1.94	(0.87)
TPC-UDS	6	0.45	0.56	(0.79)
TPC-C	6	0.50	0.73	(0.57)
TPC-B	6	1.41	1.59	(1.47)
TOPAZ	4	0.66	0.75	(1.50)
ALEPH	22	0.88	0.69	0.71
DELPHI	16	2.32	2.50	2.38
DELPHI-UDS	16	1.90	1.98	1.91
DELPHI-B	16	1.09	1.10	1.13
OPAL	22	2.05	1.87	1.98
SLD	29	1.09	0.72	1.07
SLD-UDS	29	0.80	0.60	0.73
SLD-C	29	0.97	0.80	1.10
SLD-B	29	0.44	0.43	0.43
TOTAL	378	0.99	1.14	0.93

no BB: larger uncertainties; different gluon shape and different light flavour separation
BB+LEP: comparable uncertainties; slightly different size of gluon and light flavoured quarks

Dependence upon the dataset: K^+

NNLO theory Exp.	$N_{\rm dat}$	NNFF1.0 $\chi^2/N_{\rm dat}$	no BB $\chi^2/N_{\rm dat}$	BB+LEP $\chi^2/N_{\rm dat}$
BELLE	70	0.19	(16.3)	0.37
BABAR	28	0.77	(190)	0.99
TASSO14	3	1.30	1.80	(1.23)
TASSO22	2	0.29	0.23	(0.33)
TASSO34	2	0.09	0.02	(0.04)
TPC	7	1.19	0.61	(0.45)
ALEPH	13	0.72	0.75	0.63
DELPHI	11	0.17	0.23	0.16
DELPHI-UDS	11	1.97	2.05	2.00
DELPHI-B	11	0.41	0.45	0.48
OPAL	9	2.10	2.01	2.01
SLD	21	0.77	0.76	0.77
SLD-UDS	21	1.11	1.12	1.19
SLD-C	20	0.42	0.36	0.47
SLD-B	21	0.71	0.76	0.70
TOTAL	250	0.67	0.86	0.74

no BB: larger uncertainties; different gluon shape and different light flavour separation; significant degradation in the description of BELLE and BABAR data

BB+LEP: comparable uncertainties; FFs stable; no significant degradation in fit quality; fair description of the data not included in the fit

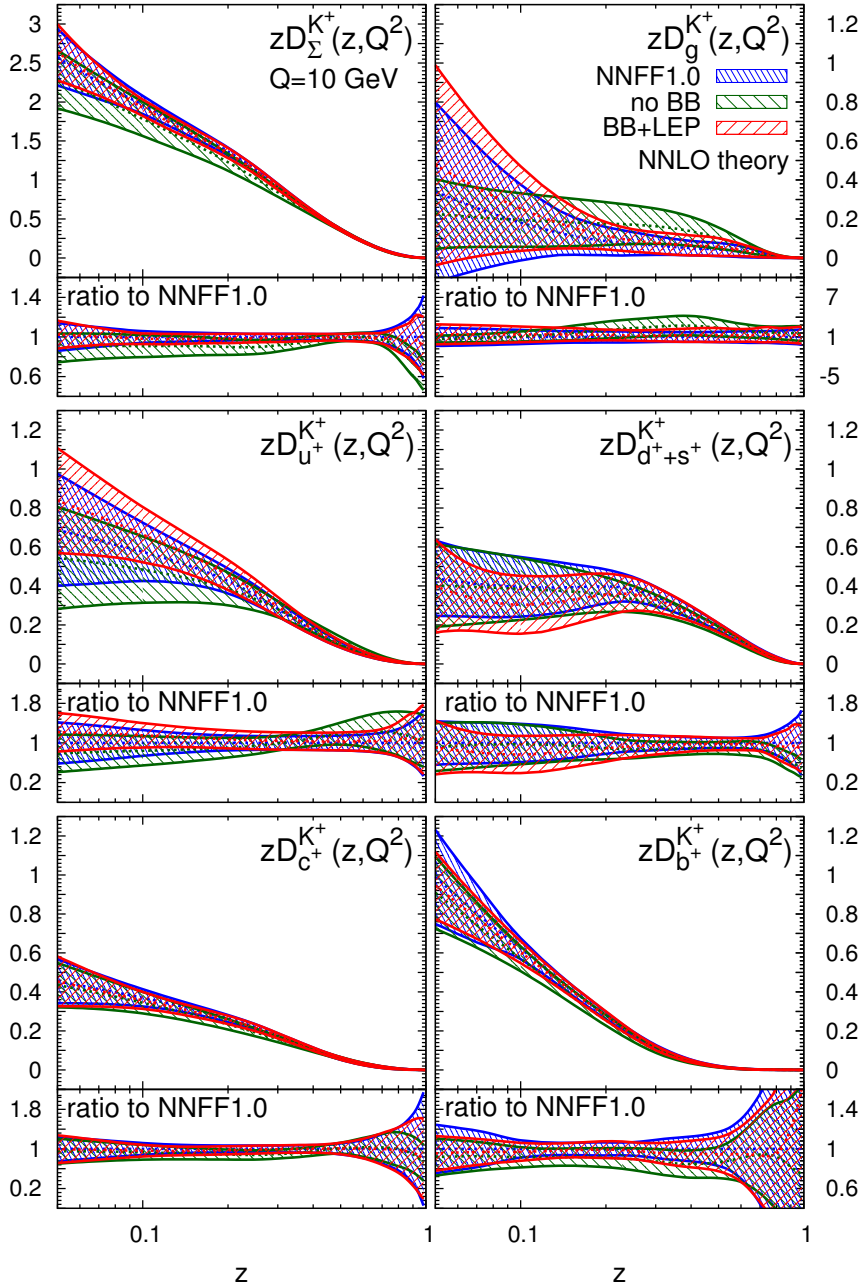

Small-z resummed Fragmentation Functions [PRD 95 (2017) 054003]

1. Double logarithmic enhancement in the splitting/SIA coefficient functions

$$P_{gi}^{(k)} \propto \alpha_s^{(k+1)} \frac{1}{z} \ln^{2k-a}(z) \quad C_{T,g}^{\mathrm{S},(k)} \propto \alpha_s^k \frac{1}{z} \ln^{2k-1-a}(z) \quad C_{L,g}^{\mathrm{S},(k)} \propto \alpha_s^k \frac{1}{z} \ln^{2k-2-a}(z)$$

$k = 0, 1, 2$ corresponds to LO, NLO, NNLO; $a = 0, 1, 2$ corresponds to LL, NLL, NNLL

2. In Mellin space double logarithms correspond to $N = 1$ poles

$$\mathcal{M}\left[\frac{\ln^{2k-1}(z)}{z}\right] \equiv \int_0^1 dx x^{N-1} \frac{\ln^{2k-1}(z)}{z} = \frac{(-1)^k (2k-1)!}{(\bar{N})^{2k}} \qquad \bar{N} = N - 1$$

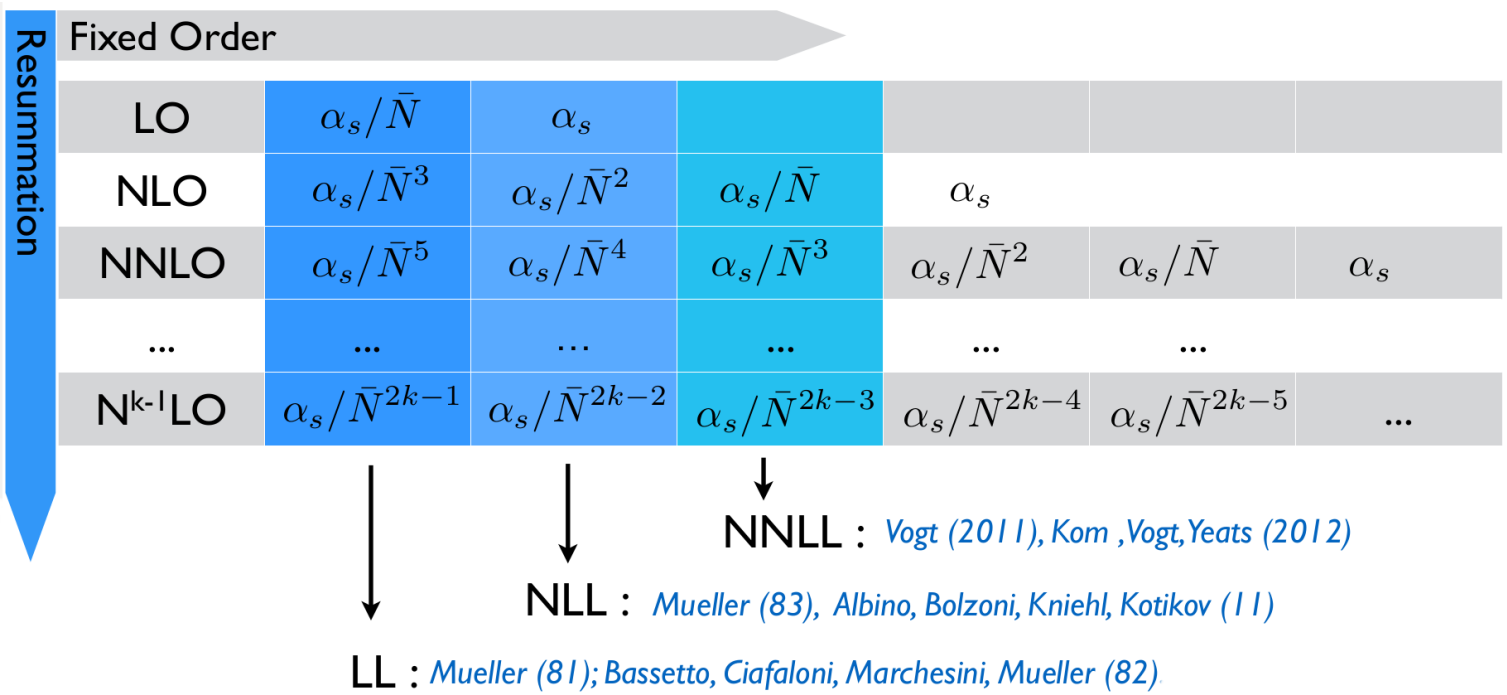

Small-z resummed Fragmentation Functions [PRD 95 (2017) 054003]

436 Total data Points:

- LEP cut (z = 0.01) due to inconsistency between OPAL and ALEPH

- TPC lower cut (z = 0.02) based on
  difference of energy fraction $z = 2\,E_h/Q$
  and three momentum fraction
  $x_p = z - 2m_h^2/(zQ^2) + \mathcal{O}(1/Q^4)$
  in c.m.s being less than at least 15%

accuracy	χ^2	χ^2/dof
LO	1260.78	2.89
NLO	354.10	0.81
NNLO	330.08	0.76
LO+LL	405.54	0.93
NLO+NNLL	352.28	0.81
NNLO+NNLL	329.96	0.76

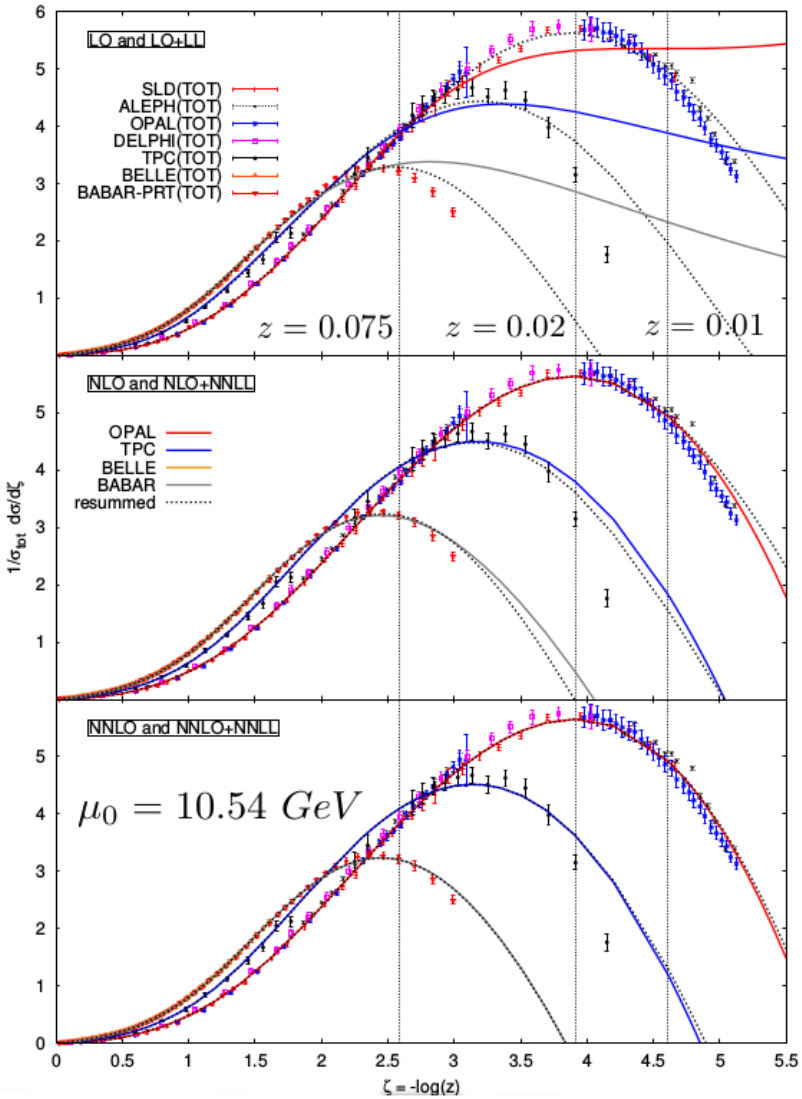

Slide: courtesy of D. P. Anderle

Small-z resummed Fragmentation Functions [PRD 95 (2017) 054003]

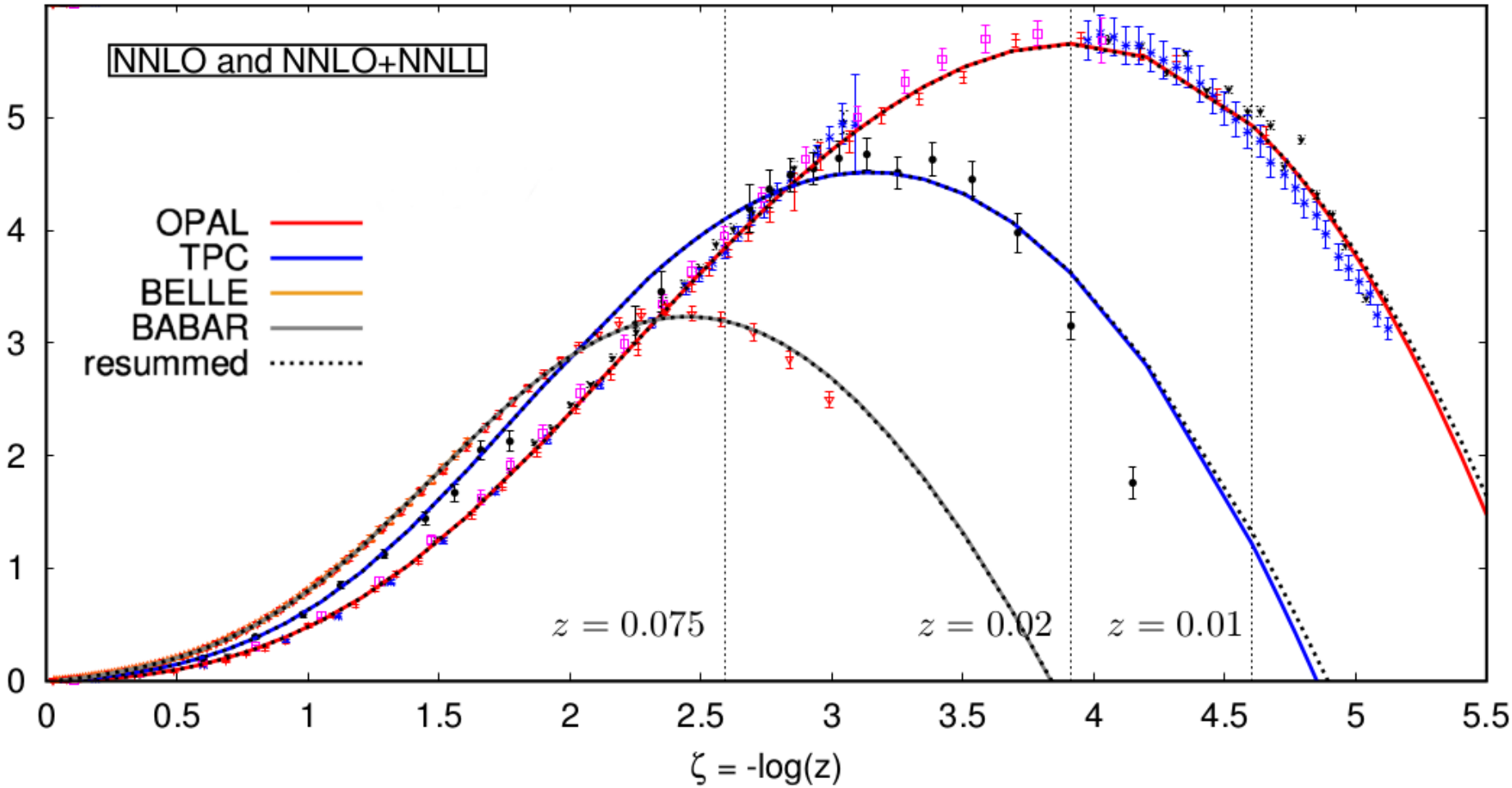

Slide: courtesy of D. P. Anderle

Dependence upon kinematic cuts

Hadron	BL		no cuts		con. cut		cut1		cut2	
	$z_{\min}^{(m_Z)}$	$z_{\min}$	$z_{\min}^{(m_Z)}$	$z_{\min}$	$z_{\min}^{(m_Z)}$	$z_{\min}$	$z_{\min}^{(m_Z)}$	$z_{\min}$	$z_{\min}^{(m_Z)}$	$z_{\min}$
$\pi^{\pm}$	0.02	0.075	0.00	0.00	0.05	0.10	0.01	0.05	0.01	0.075
$K^{\pm}$	0.02	0.075	0.00	0.00	0.10	0.20	0.05	0.10	—	—

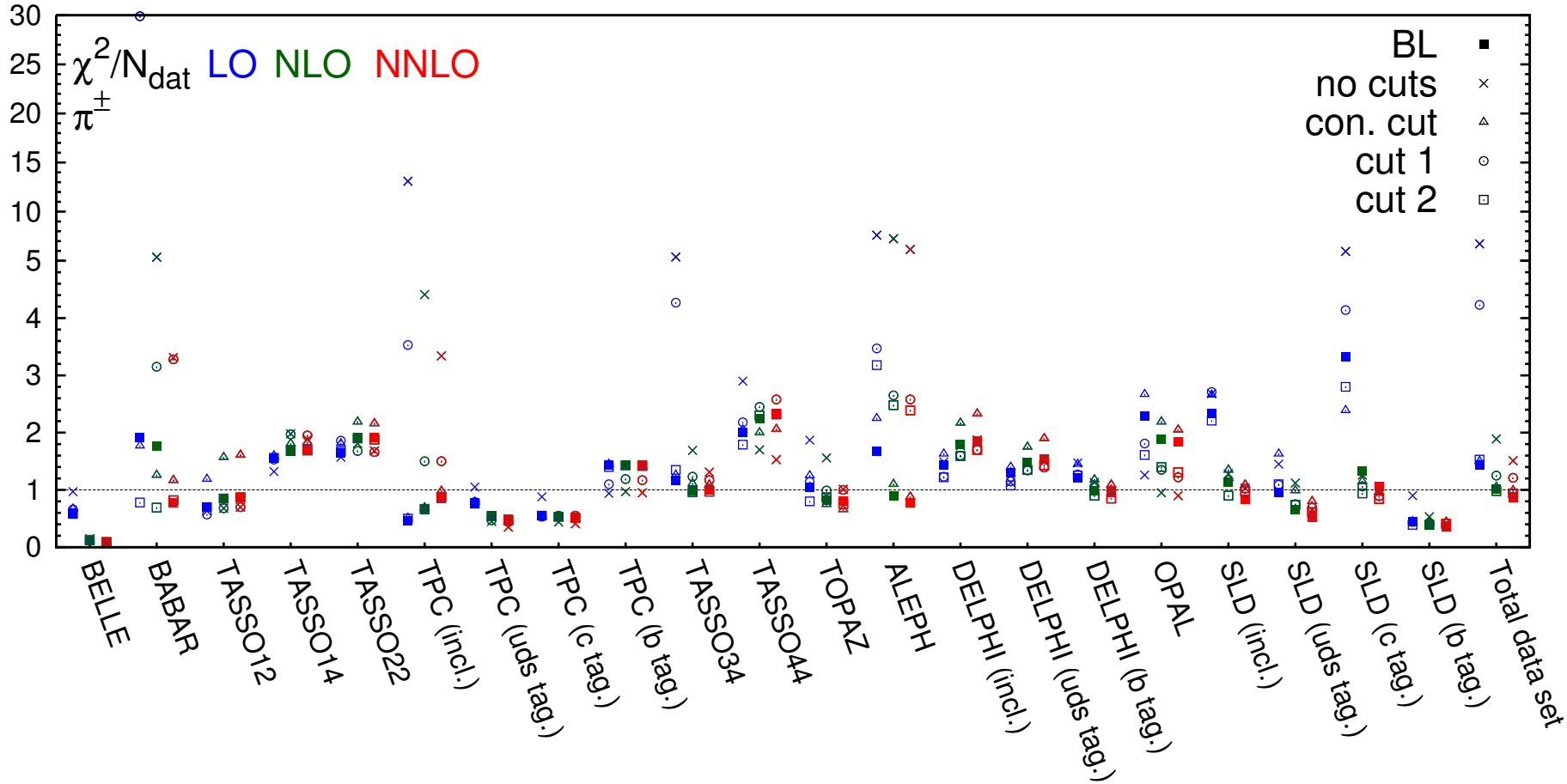

Dependence upon kinematic cuts

Hadron	BL		no cuts		con. cut		cut1		cut2	
	$z_{\min}^{(m_Z)}$	$z_{\min}$	$z_{\min}^{(m_Z)}$	$z_{\min}$	$z_{\min}^{(m_Z)}$	$z_{\min}$	$z_{\min}^{(m_Z)}$	$z_{\min}$	$z_{\min}^{(m_Z)}$	$z_{\min}$
$\pi^{\pm}$	0.02	0.075	0.00	0.00	0.05	0.10	0.01	0.05	0.01	0.075
$K^{\pm}$	0.02	0.075	0.00	0.00	0.10	0.20	0.05	0.10	—	—

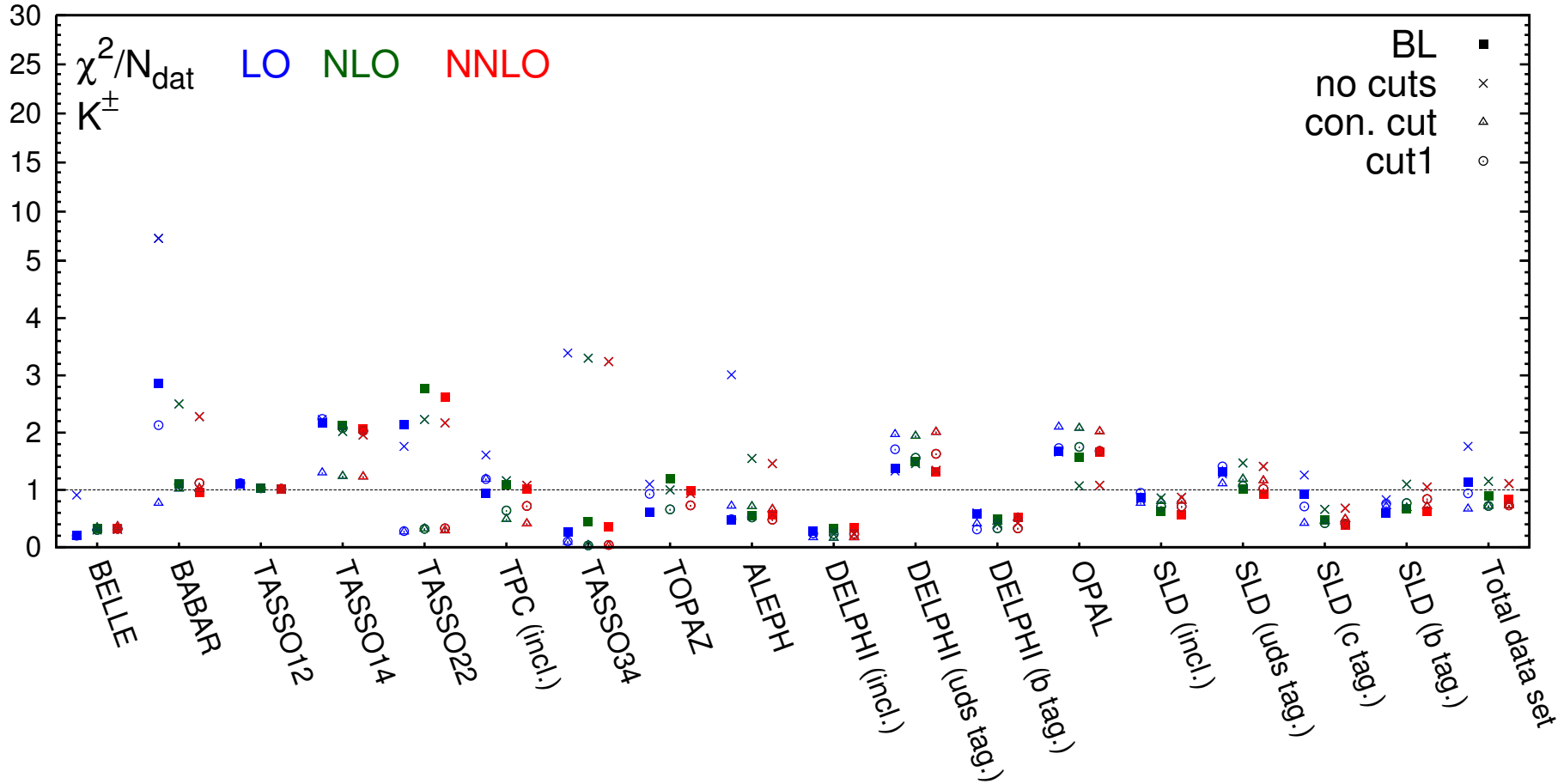

Dependence upon kinematic cuts: π^+

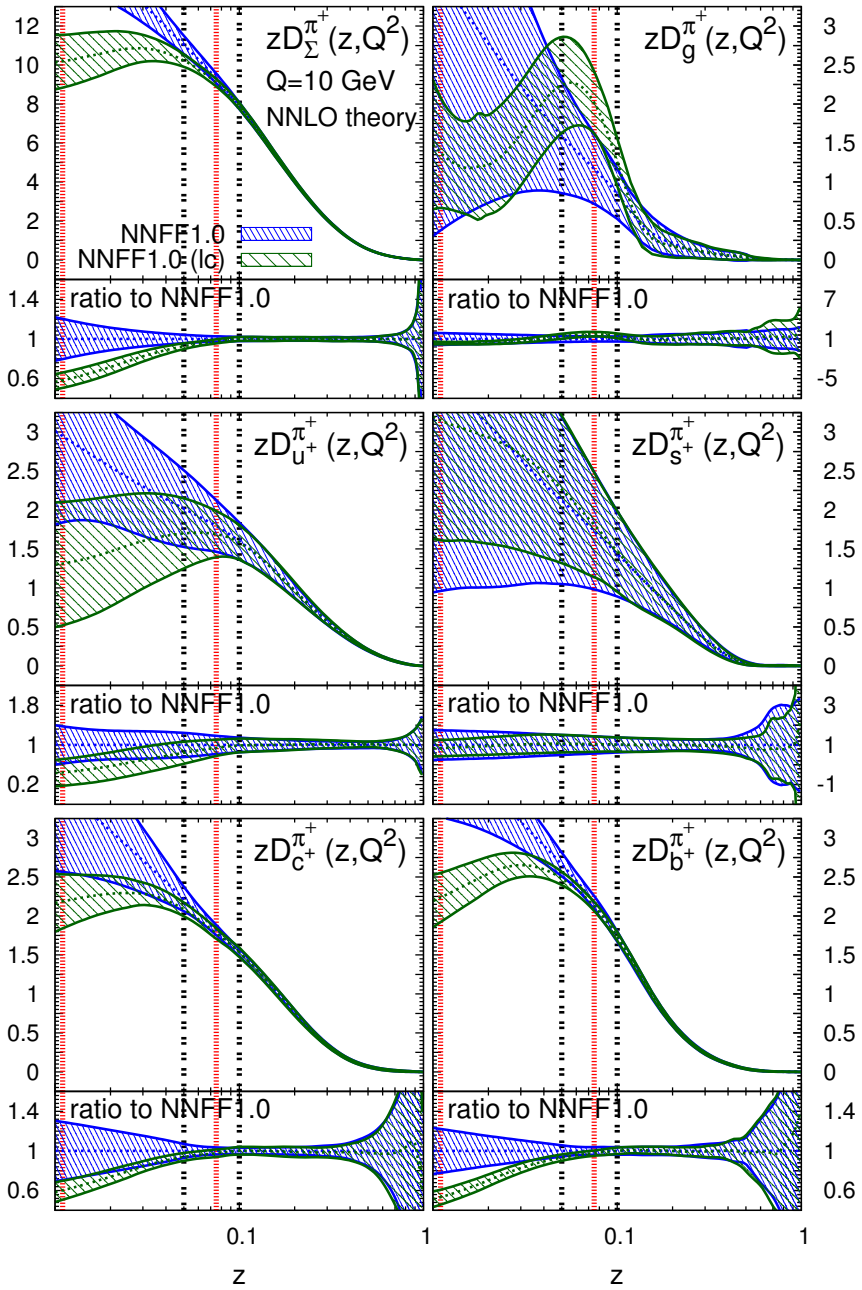

NNLO theory	NNFF1.0		NNFF1.0 (lc)	
Exp.	$N_{\rm dat}$	$\chi^2/N_{\rm dat}$	$N_{\rm dat}$	$\chi^2/N_{\rm dat}$
BELLE	70	0.08	70	0.09
BABAR	37	1.17	40	0.82
TASSO12	2	1.61	4	0.87
TASSO14	7	1.83	9	1.69
TASSO22	7	2.16	8	1.88
TASSO34	8	1.09	9	0.97
TASSO44	5	1.95	6	2.32
TPC	12	0.98	13	0.88
TPC-UDS	6	0.45	6	0.47
TPC-C	6	0.50	6	0.52
TPC-B	6	1.41	6	1.42
TOPAZ	4	0.66	5	0.75
ALEPH	22	0.88	30	2.39
DELPHI	16	2.32	22	1.70
DELPHI-UDS	16	1.90	22	1.43
DELPHI-B	16	1.09	22	0.85
OPAL	22	2.05	38	1.31
SLD	29	1.09	38	0.97
SLD-UDS	29	0.80	38	0.61
SLD-C	29	0.97	38	0.84
SLD-B	29	0.44	38	0.41
TOTAL	378	0.99	468	0.94

Slight improvement of the overall fit quality
Excellent consistency in the overlapping region
Significantly varied FF shapes at low z
Possible tensions with ALEPH at small z

Dependence upon kinematic cuts: K^+

NNLO theory		NNFF1.0		NNFF1.0 (lc)
Exp.	$N_{\rm dat}$	$\chi^2/N_{\rm dat}$	$N_{\rm dat}$	$\chi^2/N_{\rm dat}$
BELLE	70	0.19	70	0.32
BABAR	28	0.77	43	1.12
TASSO12	—	—	3	1.02
TASSO14	3	1.30	7	2.03
TASSO22	2	0.29	4	0.33
TASSO34	2	0.09	4	0.04
TPC	7	1.19	12	0.72
TOPAZ	—	—	3	0.73
ALEPH	13	0.72	18	0.48
DELPHI	11	0.17	16	0.23
DELPHI-UDS	11	1.97	16	1.63
DELPHI-B	11	0.41	16	0.33
OPAL	9	2.10	10	1.68
SLD	21	0.77	29	0.71
SLD-UDS	21	1.11	29	1.02
SLD-C	20	0.42	29	0.41
SLD-B	21	0.71	29	0.84
TOTAL	250	0.67	338	0.73

Slight deterioration of the overall fit quality
Excellent consistency in the overlapping region
Significantly varied FF shapes at low z

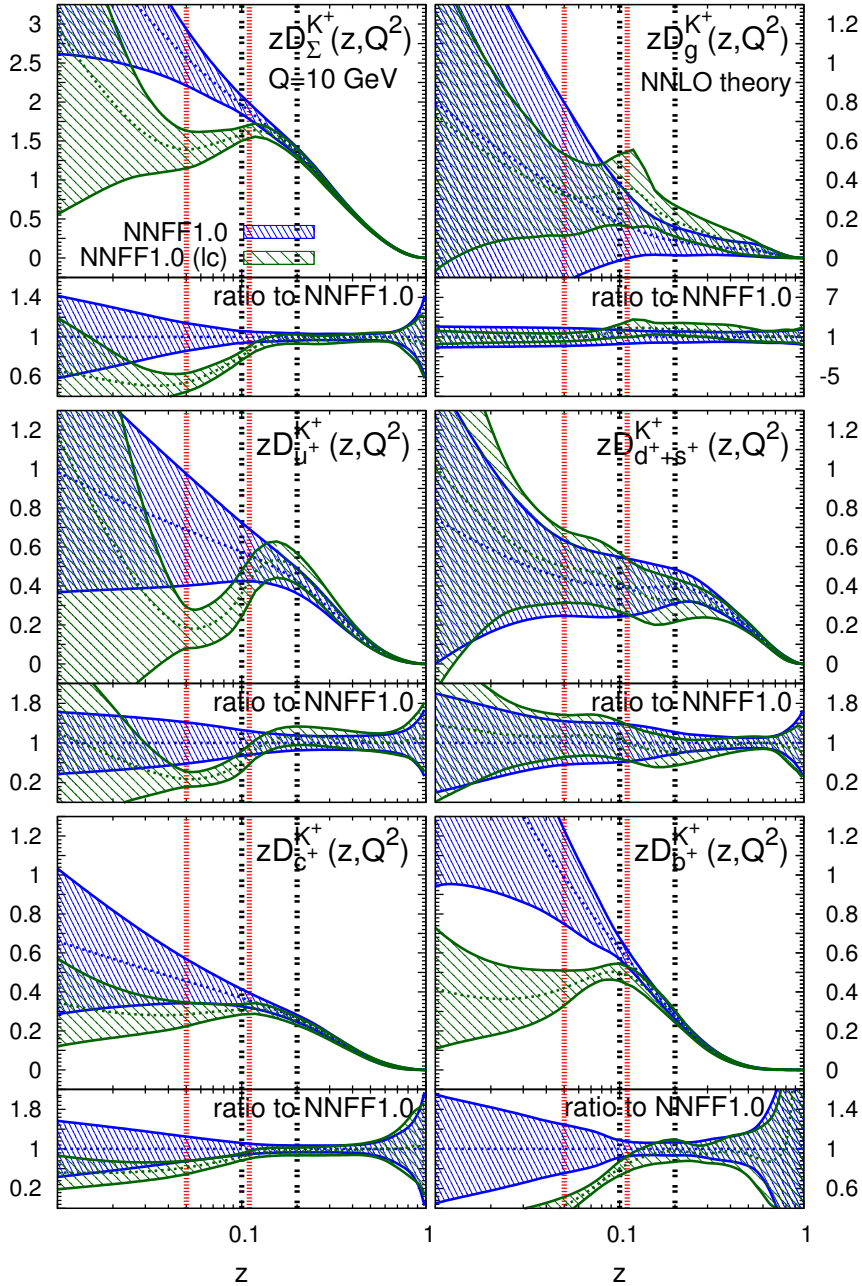

3.3 Global fits: the DEHSS analyses

Fit settings

Physical parameters: consistent with previous DSS analyses [PRD 75 (2007) 114010]

$$\alpha_s(M_Z) = 0.118,\ \alpha(M_Z) = 1/127,\ m_c = 1.43 \text{ GeV},\ m_b = 4.3 \text{ GeV}$$

Solution of DGLAP equations: numerical solution in N-space

Parametrisation: standard functional form at $Q_0 = 1$ GeV

$$D_i^h(z, Q_0) = \frac{N_i x^{a_i} (1-z)^{\beta_i} [1 + \gamma_i (1-z)^{\delta_i}]}{B[2+\alpha_i, \beta_i + 1] + \gamma_i B[2+\alpha_i, \beta_i + \delta_i + 1]}$$

PIONS

$$h = \pi^+,\ i = u^+, d+, \bar{u} = d, s^+, c^+, b^+, g$$

$D_{u^+}^{\pi^\pm} = D_{d^+}^{\pi^\pm}$ (isospin symmetry)

KAONS

$$h = K^+,$$

$$i = u^+, \bar{u} = d = \bar{d} = s, s^+, c^+, b^+, g$$

no further theoretical assumptions

assume charge conjugation, from which $D_{q^+}^{\pi^+} = D_{q^+}^{\pi^-}$

Heavy flavours: heavy-quark FFs are parametrised independently at their thresholds

Kinematic cuts: $z \to 0$: contributions $\propto \ln z$; $z \to 1$: contributions $\propto \ln(1-z)$

PIONS

$z_{\min} = 0.1$, $z_{\min} = 0.05$ ($\sqrt{s} = M_Z$)

$p_T > 5$ GeV

KAONS

$z_{\min} = 0.2$ ($\sqrt{s} = 10$ GeV), $z_{\min} = 0.1$

$p_T > 5$ GeV

Data sets and fit quality: pions and kaons

pions: $\chi^2_{\rm tot}/N_{\rm dat} = 1.19$

experiment		data type	norm. N_i	# data in fit	χ^2
TPC [48]		incl.	1.043	17	17.3
		uds tag	1.043	9	2.1
		c tag	1.043	9	5.9
		b tag	1.043	9	9.2
TASSO [49]	34 GeV	incl.	1.043	11	30.2
	44 GeV	incl.	1.043	7	22.2
SLD [19]		incl.	0.986	28	15.3
		uds tag	0.986	17	18.5
		c tag	0.986	17	16.1
		b tag	0.986	17	5.8
ALEPH [16]		incl.	1.020	22	22.9
DELPHI [17]		incl.	1.000	17	28.3
		uds tag	1.000	17	33.3
		b tag	1.000	17	10.6
OPAL [18, 20]		incl.	1.000	21	14.0
		u tag	0.786	5	31.6
		d tag	0.786	5	33.0
		s tag	0.786	5	51.3
		c tag	0.786	5	30.4
		b tag	0.786	5	14.6
BABAR [28]		incl.	1.031	45	46.4
BELLE [29]		incl.	1.044	78	44.0
HERMES [30]		π^+ (p)	0.980	32	27.8
		π^- (p)	0.980	32	47.8
		π^+ (d)	0.981	32	40.3
		π^- (d)	0.981	32	59.1
COMPASS [31] prel.		π^+ (d)	0.946	199	174.2
		π^- (d)	0.946	199	229.0
PHENIX [21]		π^0	1.112	15	15.8
STAR [33–36]	$0 \le \eta \le 1$	π^0	1.161	7	5.7
	$0.8 \le \eta \le 2.0$	π^0	0.954	7	2.7
	$\lvert\eta\rvert < 0.5$	$\pi^\pm$	1.071	8	4.3
	$\lvert\eta\rvert < 0.5$	π^+,π^-/π^+	1.006	16	17.2
ALICE [32]	7 TeV	π^0	0.766	11	27.7
TOTAL:				973	1154.6

kaons: $\chi^2_{\rm tot}/N_{\rm dat} = 1.06$

experiment	data type	norm. N_i	# data in fit	χ^2
TPC [37]	incl.	1.003	12	13.4
SLD [33]	incl.	1.014	18	17.2
	uds tag	1.014	10	31.5
	c tag	1.014	10	21.3
	b tag	1.014	10	11.9
ALEPH [30]	incl.	1.026	13	29.7
DELPHI [31]	incl.	1.000	12	6.9
	uds tag	1.000	12	13.1
	b tag	1.000	12	11.0
OPAL [34]	*u* tag	0.778	5	9.6
	d tag	0.778	5	7.7
	s tag	0.778	5	23.4
	c tag	0.778	5	42.5
	b tag	0.778	5	16.9
BABAR [17]	incl.	1.077	45	30.6
BELLE [18]	incl.	0.996	78	15.6
HERMES [19]	K^+ (p) Q^2	0.843	36	61.9
	K^- (p) Q^2	0.843	36	29.6
	K^+ (p) x	1.135	36	75.8
	K^- (p) x	1.135	36	42.1
	K^+ (d) Q^2	0.845	36	44.7
	K^- (d) Q^2	0.845	36	41.9
	K^+ (d) x	1.095	36	48.9
	K^- (d) x	1.095	36	44.4
COMPASS [22]	K^+ (d)	0.996	309	285.8
	K^- (d)	0.996	309	265.1
STAR [24]	K^+,K^-/K^+	1.088	16	7.6
ALICE [23] 2.76 TeV	K/π	0.985	15	21.6
TOTAL:			1194	1271.7

Data/theory comparison: SIDIS multiplicities (pions)

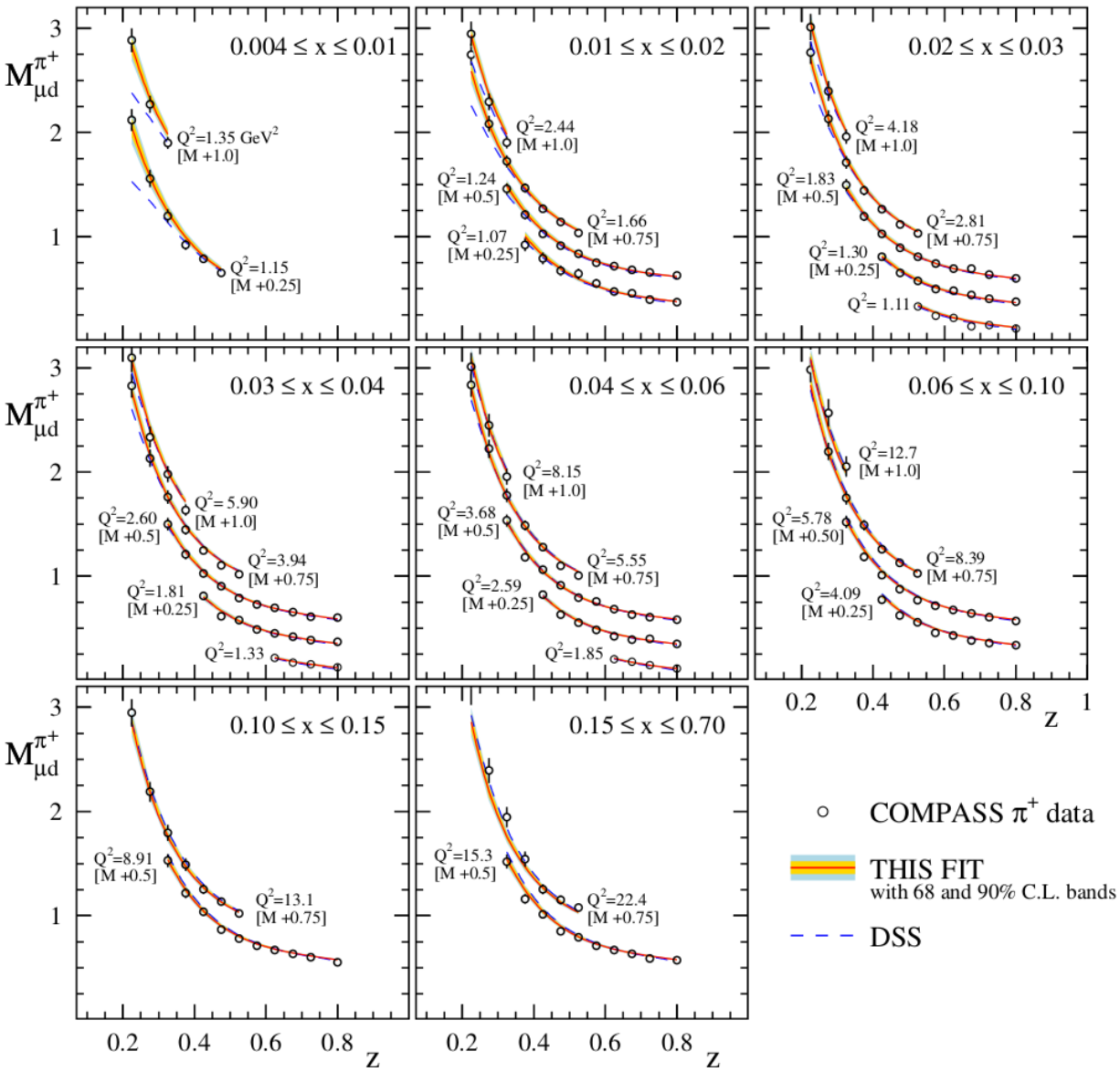

Data/theory comparison: SIDIS multiplicities (pions)

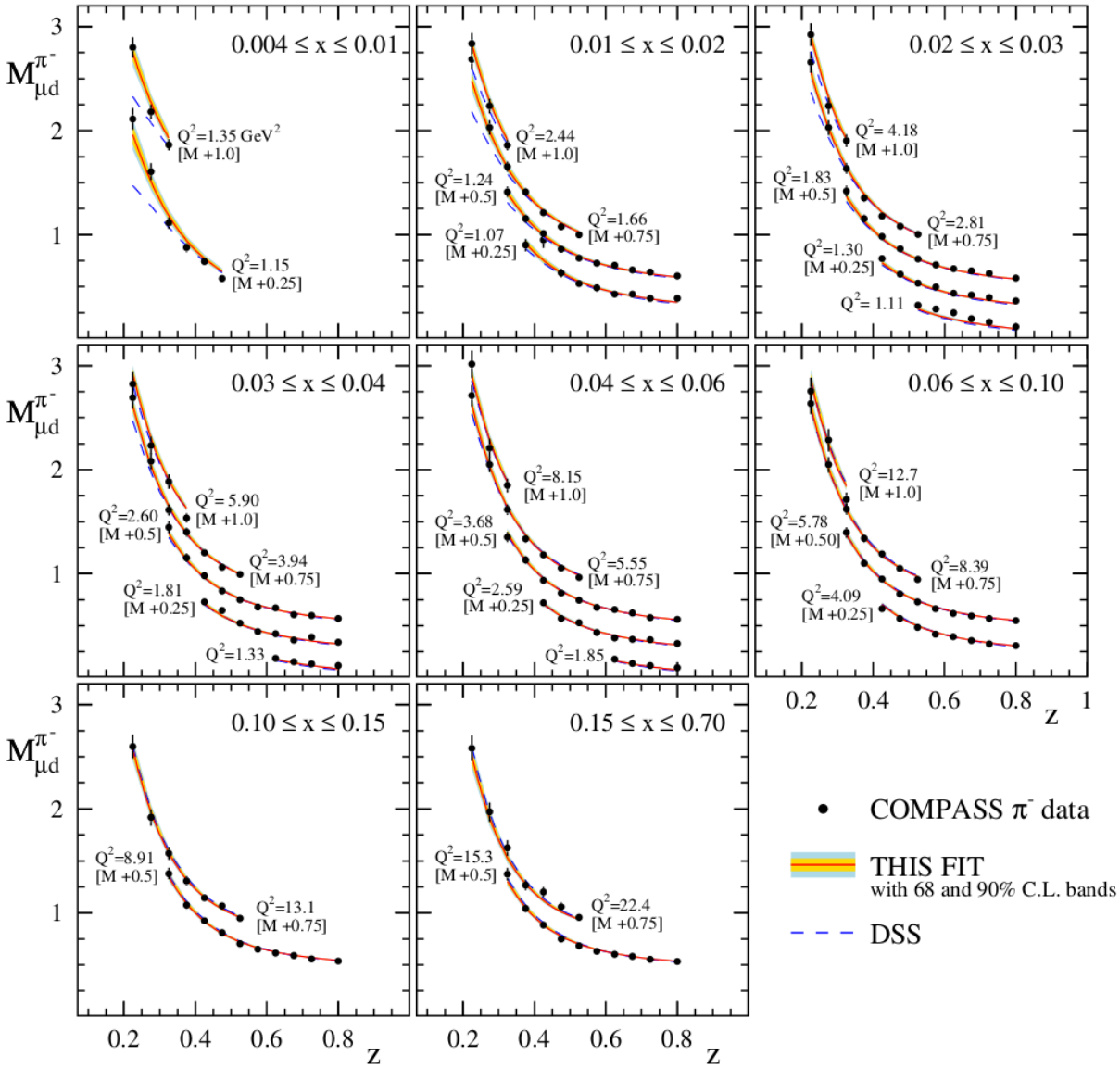

Data/theory comparison: SIDIS multiplicities (kaons)

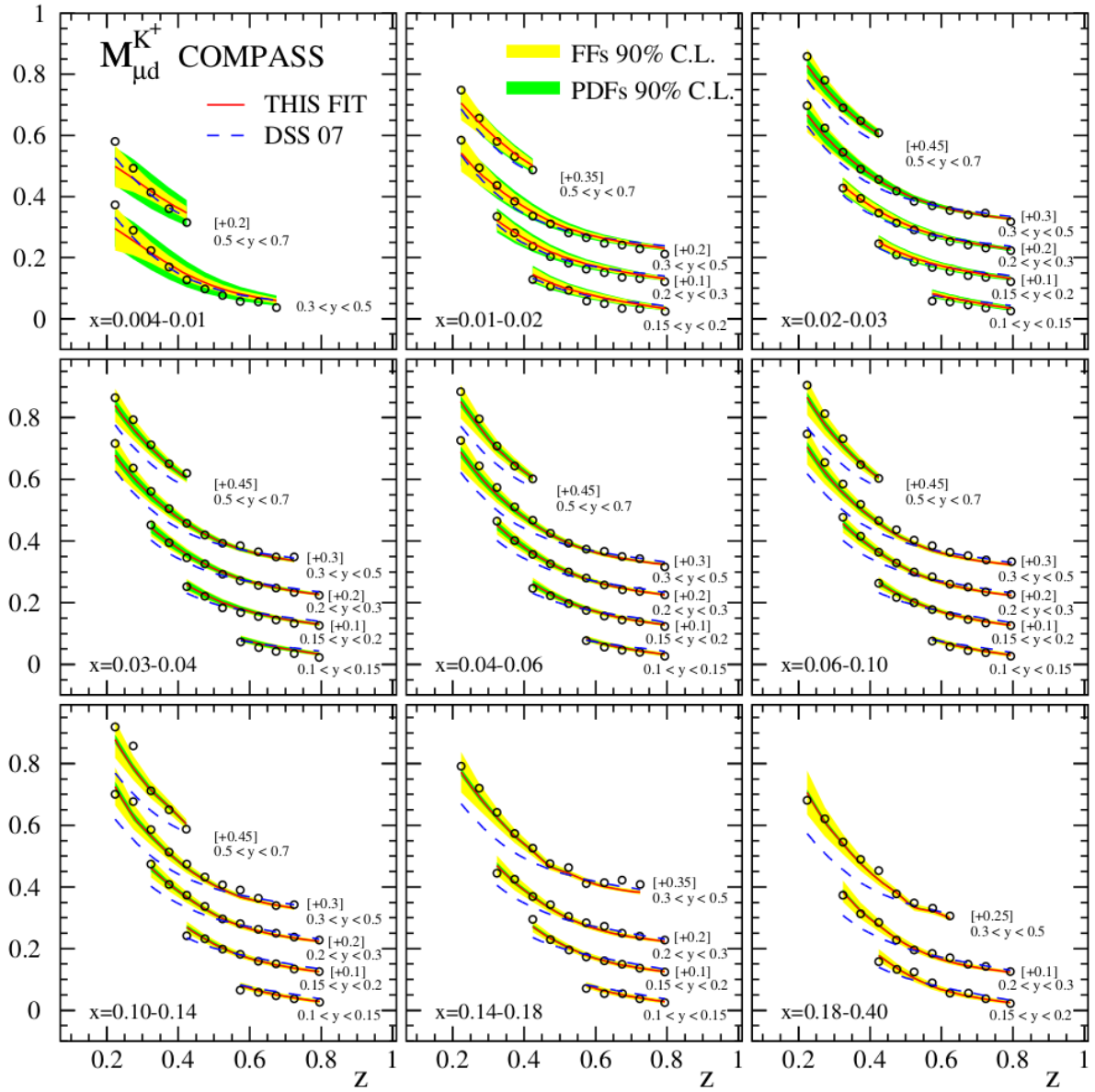

Data/theory comparison: SIDIS multiplicities (kaons)

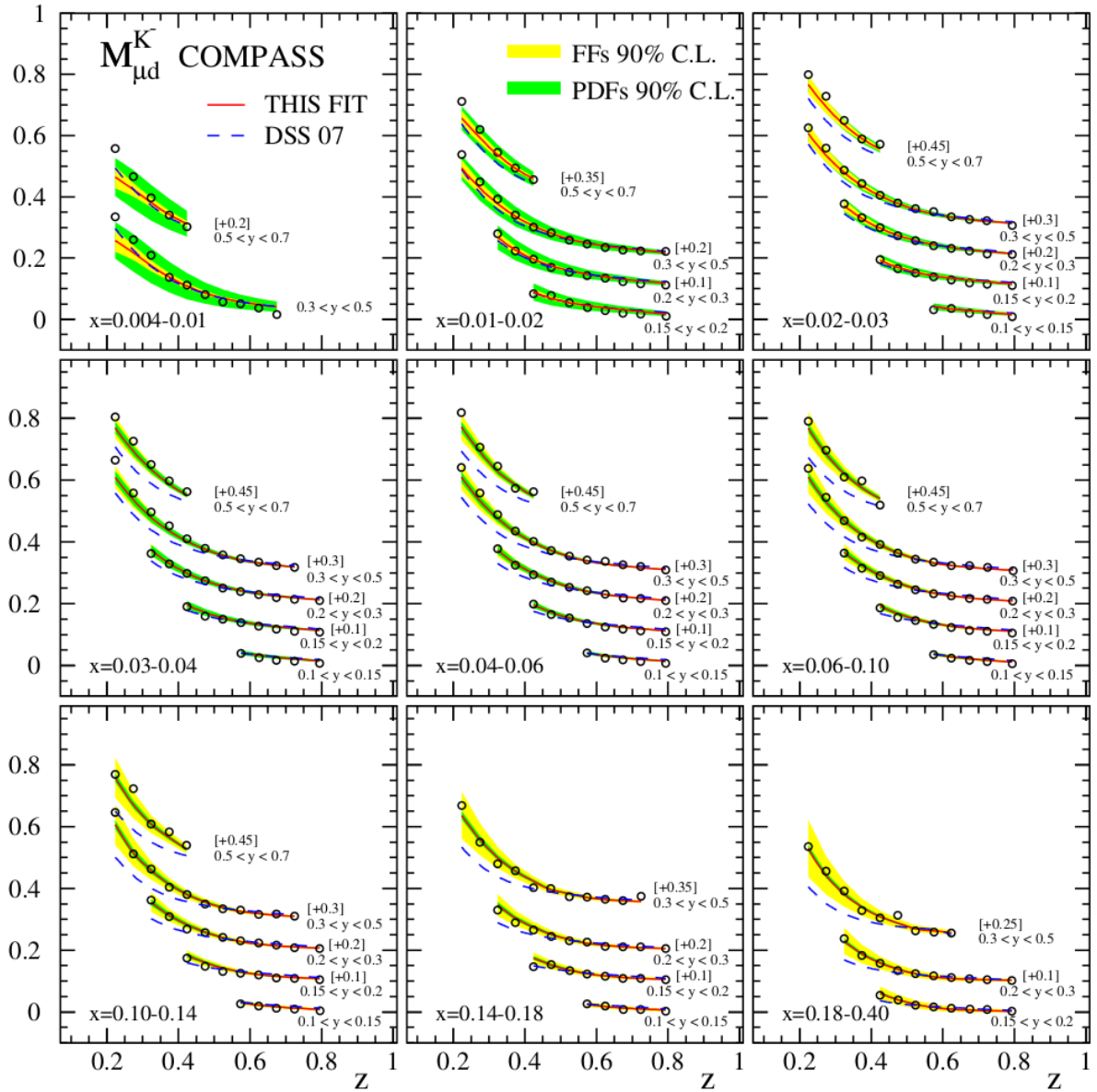

Data/theory comparison: pp data (pions)

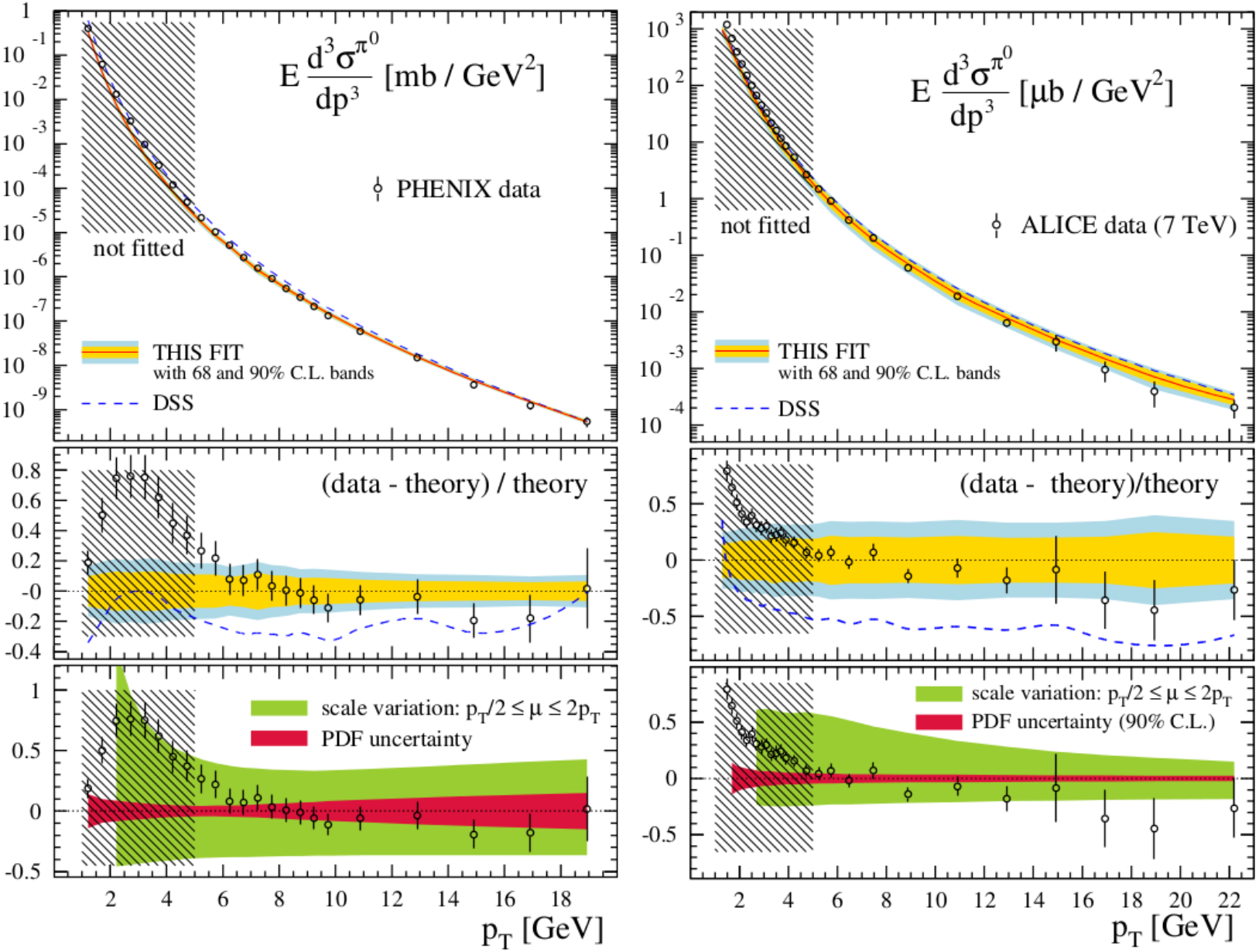

Data/theory comparison: pp data (kaons)

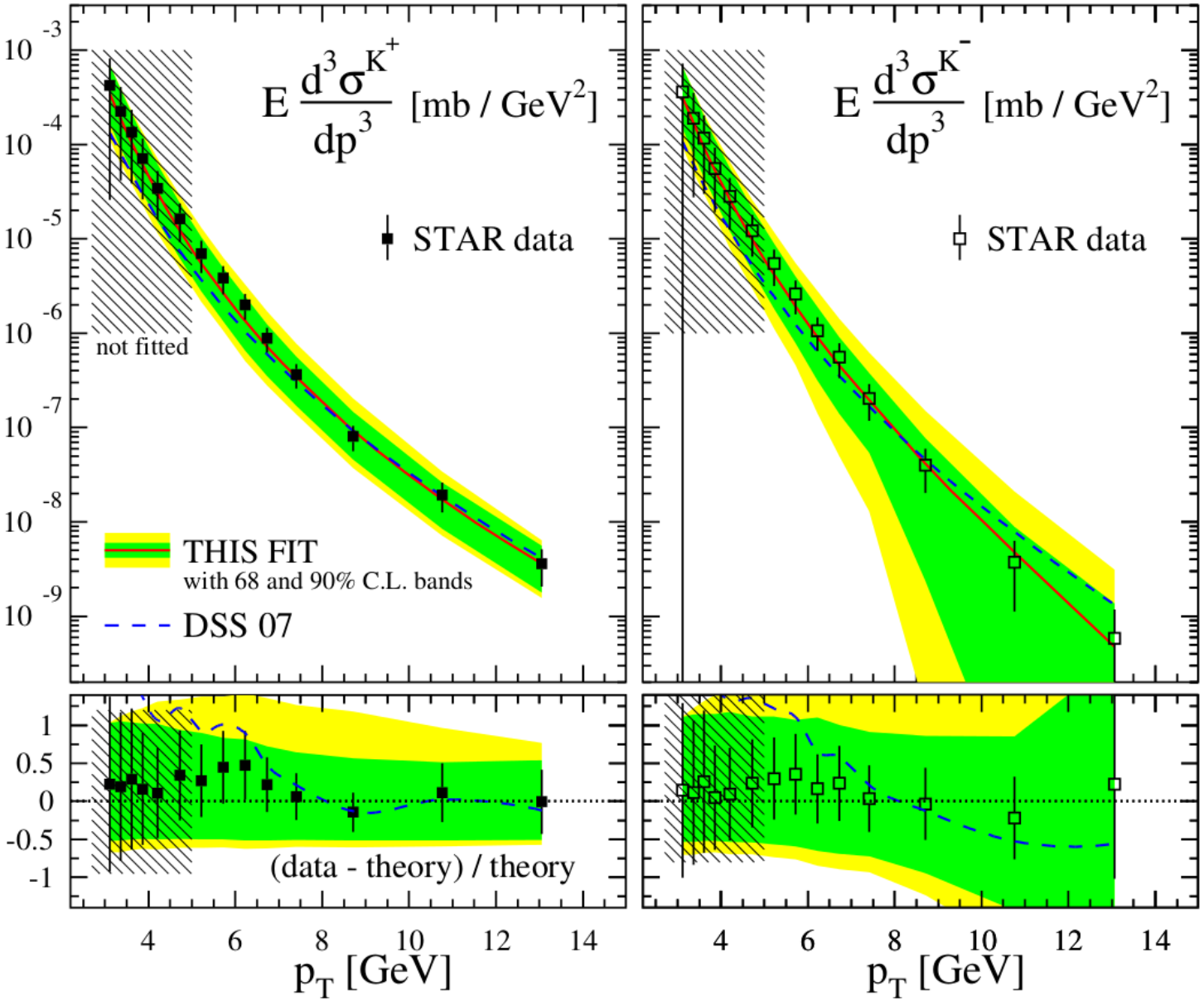

Comparison among various FF determinations (pions)

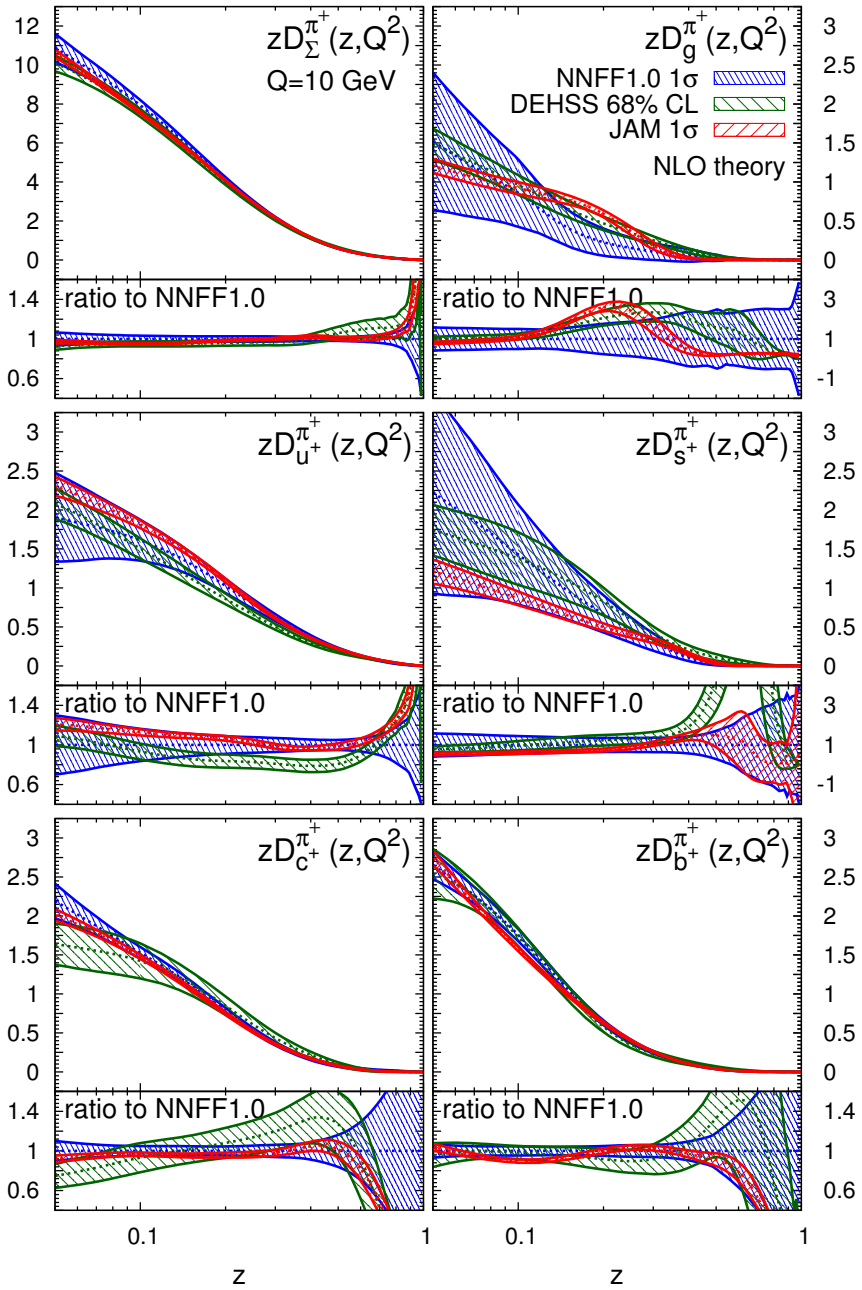

DEHSS [PRD 91 (2015) 014035]
(+SIDIS +PP)

JAM [PRD 94 (2016) 114004]
(almost same dataset as NNFF1.0)

$D_\Sigma^{\pi^+}$: excellent mutual agreement
both c.v. and unc. (bulk of the dataset)

$D_g^{\pi^+}$: slight disagreement
different shapes, larger uncertainties
DEHSS: data; JAM: parametrisation

$D_{u^+}^{\pi^+}$, $D_{s^+}^{\pi^+}$: good overall agreement
excellent with JAM, though larger uncertainties
slight different shape w.r.t. DHESS (dataset)

$D_{c^+}^{\pi^+}$, $D_{b^+}^{\pi^+}$: good overall agreement
excellent with JAM, same uncertainties
slight different shape w.r.t. DHESS (dataset)

Comparison among various FF determinations (kaons)

DEHSS [PRD 95 (2017) 094019]
(+SIDIS +PP)

JAM [PRD 94 (2016) 114004]
(almost same dataset as NNFF1.0)

$D_{\Sigma}^{\pi^+}$: excellent agreement (both c.v. and unc.)
bulk of the dataset

$D_{g}^{\pi^+}$: good mutual agreement
similar shapes, larger uncertainties
DEHSS: data; JAM: parametrisation

$D_{u^+}^{\pi^+}$: mutual sizable disagreement
differences in dataset and parametrisation
comparable uncertainties in the data region

$D_{d^+}^{\pi^+} + D_{s^+}^{\pi^+}$: fair mutual agreement
differences in dataset and parametrisation
comparable uncertainties in the data region

$D_{c^+}^{\pi^+}$, $D_{b^+}^{\pi^+}$: excellent mutual agreement
uncertainties similar to JAM
DHESS shows inflated uncertainties

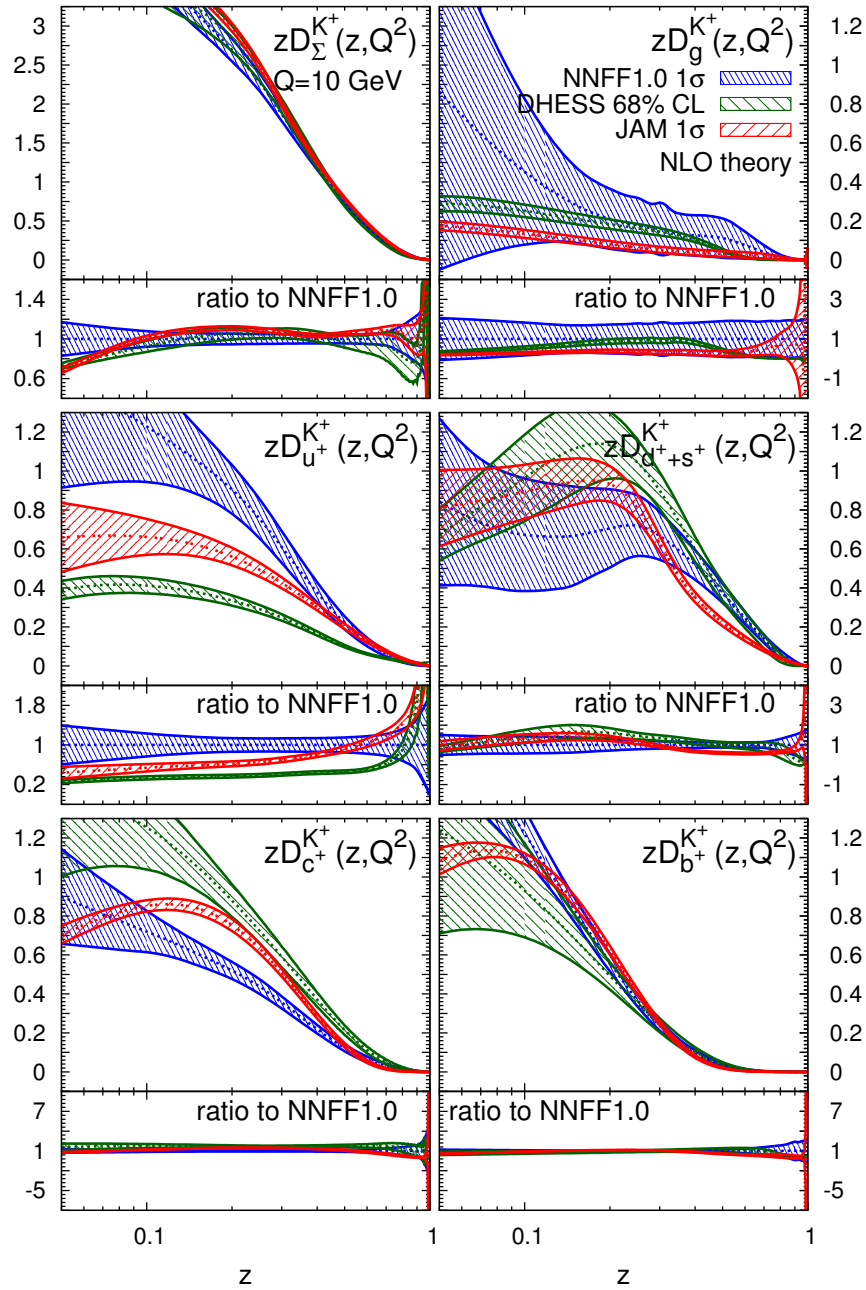

Impact of different flavours schemes (pions)

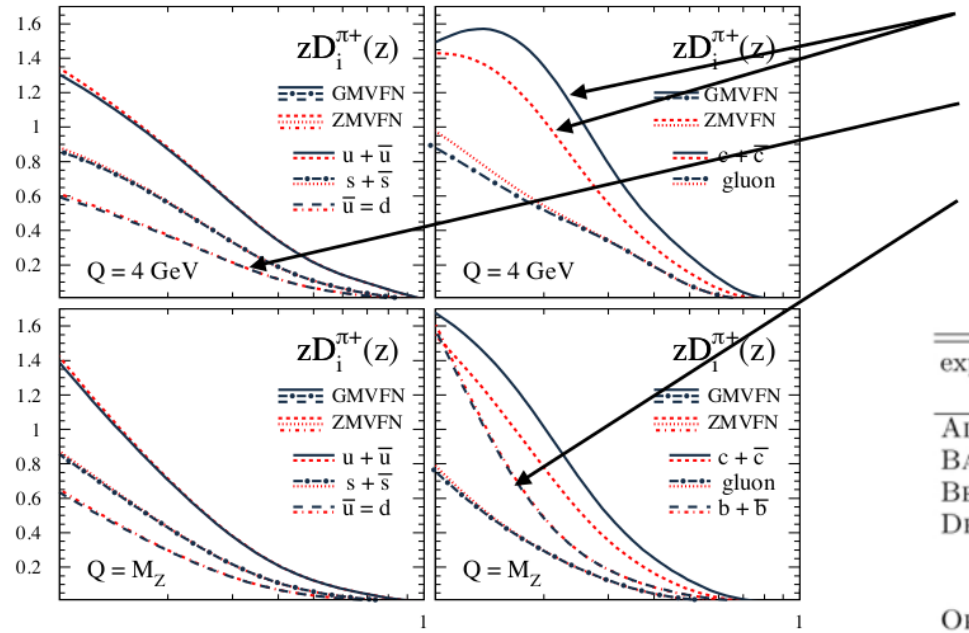

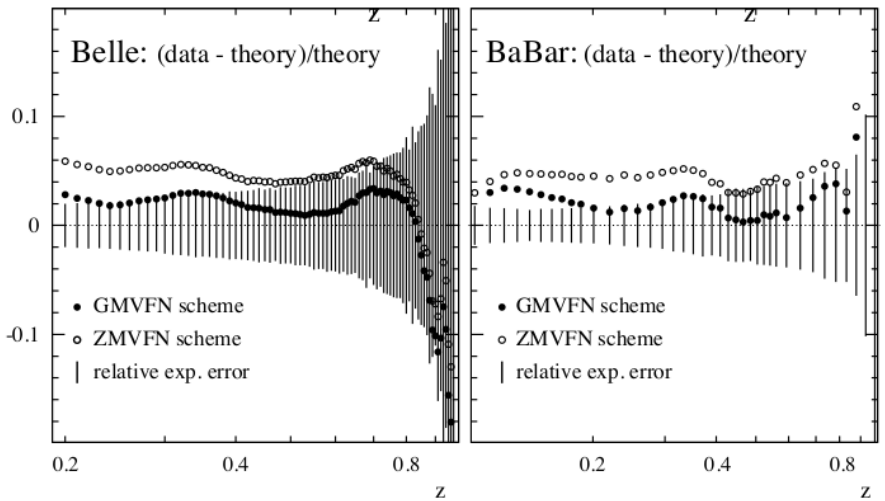

charm changes significantly

light flavors constrained by sidis

bottom constrained by high Q

experiment	data type	# data in fit	ZMVFN N_i	ZMVFN χ^2	GMVFN N_i	GMVFN χ^2
ALEPH [23]	incl.	22	0.968	21.6	0.994	23.3
BABAR [13]	incl.	39	1.019	76.7	1.002	58.2
BELLE [14]	incl.	78	1.044	19.5	1.019	11.0
DELPHI [24]	incl.	17	0.978	6.7	1.003	9.3
	uds tag	17	0.978	20.8	1.003	9.5
	b tag	17	0.978	10.5	1.003	7.8
OPAL [25]	incl.	21	0.946	27.9	0.970	15.9
SLD [26]	incl.	28	0.938	28.0	0.963	9.5
	uds tag	17	0.938	21.3	0.963	11.3
	c tag	17	0.938	34.0	0.963	19.8
	b tag	17	0.938	11.1	0.963	9.9
TPC [27]	incl.	17	0.997	31.7	1.006	27.9
	uds tag	9	0.997	2.0	1.006	2.0
	c tag	9	0.997	5.9	1.006	4.3
	b tag	9	0.997	9.6	1.006	10.9
COMPASS [28]	$\pi^{\pm}$ (d)	398	1.003	378.7	1.008	382.9
HERMES [29]	$\pi^{\pm}$ (p)	64	0.981	74.0	0.986	69.9
	$\pi^{\pm}$ (d)	64	0.980	107.3	0.985	103.7
PHENIX [30]	π^0	15	1.174	14.3	1.167	14.4
STAR [31]	$\pi^{\pm}$, π^0	38	1.205	31.2	1.202	33.8
ALICE [32]	π^0	11	0.696	33.3	0.700	31.2
TOTAL:		924		966.4		875.8

Slide: courtesy of R. Sassot

3.4 Interlude: the helicity structure of the proton

Where does the proton angular momentum come from?

$$a_0 = \left\langle P;S|\hat{J}^z_\Sigma(\mu^2)|P;S\right\rangle \xrightarrow{\text{naive p.m.}} 2\langle S^{q+\bar{q}}_z\rangle \simeq 1$$

($a_0 \sim 0.6$ including relativistic effects [NPB 337 (1990) 509])

EMC 1988 $a_0 = 0.098 \pm 0.076 \pm 0.113$ [PLB 206 (1998) 364; NPB 328 (1989) 1]

An anomalous gluon contribution to the singlet axial charge [PLB 212 (1988) 391]

$$a_0 = \left\langle P;S|\hat{J}^z_\Sigma(\mu^2)|P;S\right\rangle \overset{\overline{\text{MS}}}{=} \Delta\Sigma(\mu^2) - n_f\frac{\alpha_s(\mu^2)}{2\pi}\Delta G(\mu^2) \qquad \Delta G(\mu^2) \propto \left[\alpha_s(\mu^2)\right]^{-1}$$

The gluon does not decouple in the asymptotic limit

A realization of the proton's total angular momentum decomposition [NPB 337 (1990) 509]

$$\mathcal{J}(\mu^2) = \sum_f \left\langle P;S|\hat{J}^z_f(\mu^2)|P;S\right\rangle = \frac{1}{2} = \frac{1}{2}\Delta\Sigma(\mu^2) + \Delta G(\mu^2) + \mathcal{L}_q(\mu^2) + \mathcal{L}_g(\mu^2)$$

The decomposition is not unique

What should be the decompositions that lead to gauge-invariant, physically meaningful terms (and in which sense these are measurable) are discussed in [Phys.Rept. 541 (2014) 163]

Here I focus on $\Delta\Sigma$ and Δg

$$\Delta\Sigma(\mu^2) = \sum_q^{n_f}\int_0^1 [\Delta q(x,\mu^2) + \Delta\bar{q}(x,\mu^2)] \qquad \Delta G(\mu^2) = \int_0^1 dx \Delta g(x,\mu^2)$$

Data: spin asymmetries

PROCESS	OBSERVED ASYMMETRIES	SUBPROCESSES	PROBED PDFS
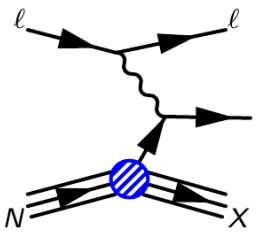 DIS $\ell^\pm + N \to \ell^\pm + X$	$A_1 \approx \frac{\sum_q \Delta q(x) + \Delta\bar{q}(x)}{\sum_{q'} q'(x) + \bar{q}'(x)}$	$\gamma^* q \to q$	$\Delta q + \Delta\bar{q}$ Δg (NLO)
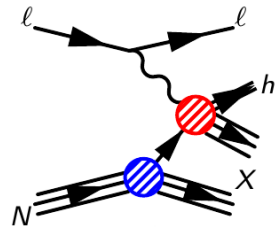 SIDIS $\ell^\pm + N \to \ell^\pm h + X$	$A_1^h \approx \frac{\sum_q \Delta q(x) \otimes D_q^h(z)}{\sum_{q'} q'(x) \otimes D_{q'}^h(z)}$	$\gamma^* q \to q$	$\Delta u\ \Delta\bar{u}$ $\Delta d\ \Delta\bar{d}$ Δg (NLO)
	$A_{LL}^{\gamma N \to D_0 X} \approx \frac{\Delta g \otimes D_c^{D^0}(z)}{g(x) \otimes D_c^{D^0}(z)}$	$\gamma^* g \to c\bar{c}$	Δg
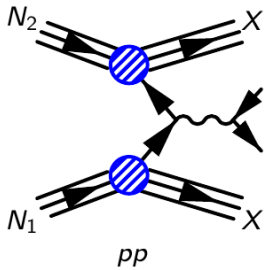 pp $N_1 + N_2 \to A + X$ $A = jet(s), W^\pm, \pi$	$A_{LL}^{jet} \approx \frac{\sum_{a,b=q,\bar{q},g} \Delta f_a(x_1) \otimes \Delta f_b(x_2)}{\sum_{a,b,c=q,\bar{q},g} f_a(x_1) \otimes f_b(x_2)}$	$gg \to qg$ $qg \to qg$	Δg
	$A_L^{W^+} \approx \frac{\Delta u(x_1)\bar{d}(x_2) - \Delta\bar{d}(x_1)u(x_2)}{u(x_1)\bar{d}(x_2) + \bar{d}(x_1)u(x_2)}$	$u_L \bar{d}_R \to W^+$ $d_L \bar{u}_R \to W^+$	$\Delta u\ \Delta\bar{u}$ $\Delta d\ \Delta\bar{d}$
	$A_{LL}^h \approx \frac{\sum_{a,b,c=q,\bar{q},g} \Delta f_a(x_1) \otimes \Delta f_b(x_2) \otimes D_c^h(z)}{\sum_{a,b,c=q,\bar{q},g} f_a(x_1) \otimes f_b(x_2) \otimes D_c^h(z)}$	$gg \to qg$ $qg \to qg$	Δg

Overview of available polarised PDF sets

	DSSV	NNPDF	JAM	LSS
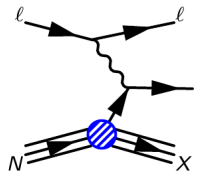 DIS	☑	☑	☑	☑
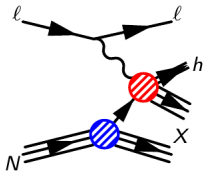 SIDIS	☑	☒	☒	☑
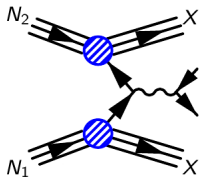 pp	☑ (jets, π^0)	☑ (jets, $W^\pm$)	☒	☒
statistical treatment	Lagr. mult. $\Delta\chi^2/\chi^2 = 2\%$	Monte Carlo	Hessian $\Delta\chi^2 = 1$	Hessian $\Delta\chi^2 = 1$
parametrization	polynomial (23 pars)	neural network (259 pars)	polynomial (10 pars)	polynomial (20 pars)
features	global fit	minimally biased fit	large-x effects	higher-twist effects
latest update	PRL 113 (2014) 012001	NP B887 (2014) 276	PR D89 (2014) 034025	PR D91 (2015) 054017

+ some others: AAC [NP B813 (2009) 106] BB [NP B841 (2010) 205], AKS [PR D89 (2014) 034006], ...

Theory: theoretical constraints

1. Polarized PDFs must lead to positive cross sections
   - at LO, polarised PDFs are bounded by their unpolarised counterparts

$$|\Delta f(x,\mu^2)| \leq f(x,\mu^2)$$

   - beyond LO, other relations hold, but are of limited effect [NP B534 (1998) 277]

2. Polarized PDFs must be integrable
   - *i.e.* require that the axial matrix elements of the nucleon are finite

$$\langle P,S|\bar{\psi}_q \gamma^\mu \gamma_5 \psi_q|P,S\rangle \longrightarrow \text{finite for each flavor } q$$

3. Assume SU(2) and SU(3) symmetry
   - relate the octet of axial-vector currents to β-decay of spin-$1/2$ hyperons

$$a_3 = \int_0^1 dx\, \Delta T_3 = 1.2701 \pm 0.0025 \qquad a_8 = \int_0^1 dx\, \Delta T_8 = 0.585 \pm 0.025 \qquad \text{[PDG 2014]}$$

$$\Delta T_3 = (\Delta u + \Delta\bar{u}) - (\Delta d + \Delta\bar{d}) \qquad \Delta T_8 = (\Delta u + \Delta\bar{u}) + (\Delta d + \Delta\bar{d}) - 2(\Delta s + \Delta\bar{s})$$

   - note: violations of SU(3) symmetry are advocated in the literature [ARNPS 53 (2003) 39]

Kinematic coverage and fit quality

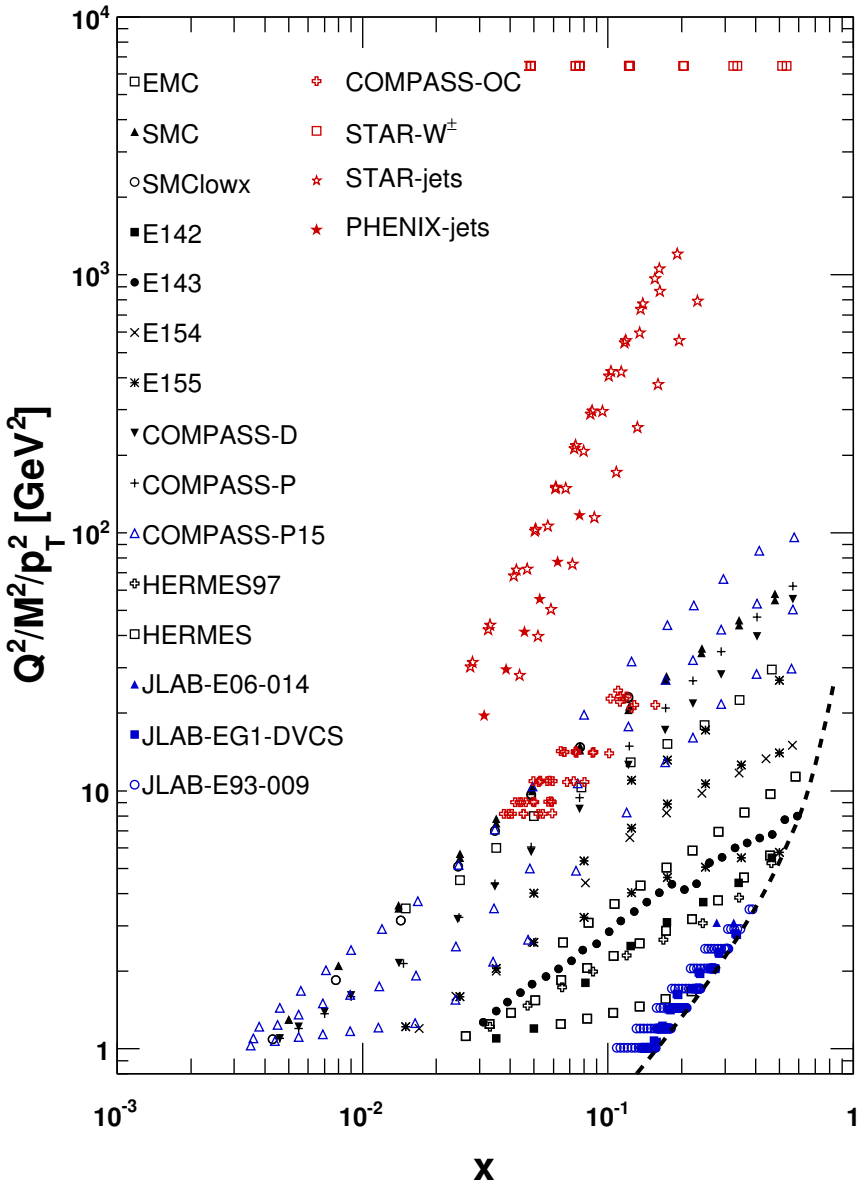

EXPERIMENT	$N_{\rm dat}$	$\chi^2/N_{\rm dat}$ 1.0	1.1	1.2
EMC	10	0.44	0.43	0.43
SMC	24	0.93	0.90	0.92
SMClowx	16	0.97	0.97	0.94
E142	8	0.67	0.66	0.55
E143	50	0.64	0.67	0.63
E154	11	0.40	0.45	0.34
E155	40	0.89	0.85	0.98
COMPASS-D	15	0.65	0.70	0.57
COMPASS-P	15	1.31	1.38	0.93
HERMES97	8	0.34	0.34	0.23
HERMES	56	0.79	0.82	0.69
COMPASS-P-15	51	0.98*	0.99*	0.65
JLAB-E93-009	148	1.26*	1.23*	0.94
JLAB-EG1-DVCS	18	0.45*	0.59*	0.29
JLAB-E06-014	2	2.81*	3.20*	1.33
TOTAL DIS		0.77	0.78	0.74
COMPASS (OC)	45	1.22*	1.22	1.22
STAR (jets)	41	—	1.05	1.06
PHENIX (jets)	6	—	0.24	0.24
STAR-A_L	24	—	1.05	1.05
STAR-A_{LL}	12	—	0.95	0.94
TOTAL		0.77	1.05	1.01

* data set not included in the corresponding fit

Polarized PDFs from inclusive DIS: status 2013

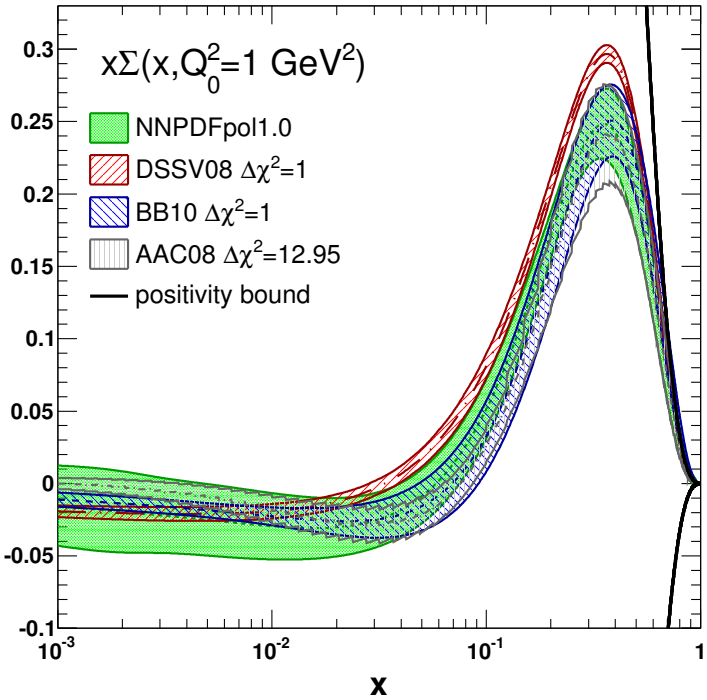

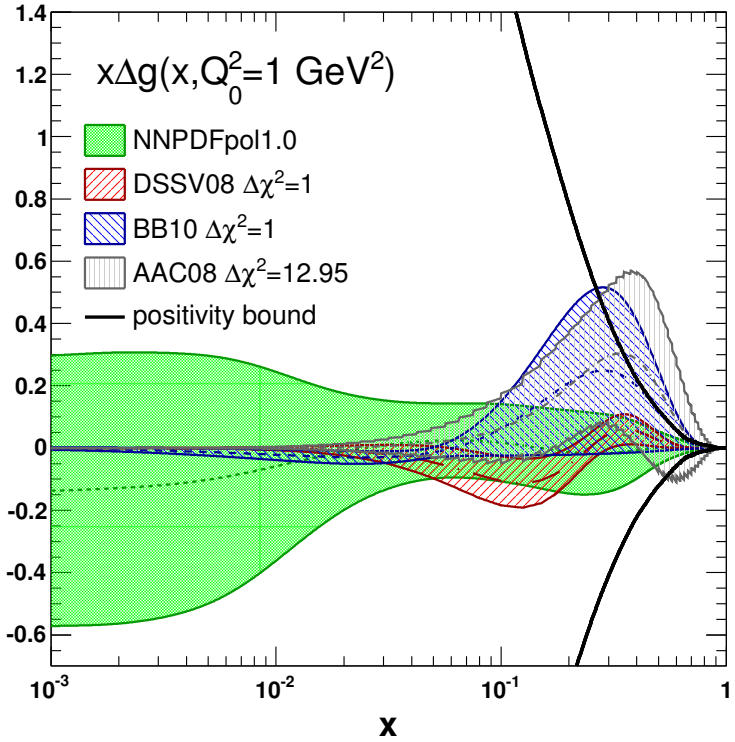

$$\int_{0.001}^{1} dx \Delta\Sigma(x, Q_0^2) = +0.25 \pm 0.09$$

$$\int_{0}^{1} dx \Delta\Sigma(x, Q_0^2) = +0.22 \pm 0.20$$

$$\int_{0.001}^{1} dx \Delta g(x, Q_0^2) = -0.26 \pm 0.19$$

$$\int_{0}^{1} dx \Delta g(x, Q_0^2) = -1.2 \pm 4.2$$

Two new analyses in 2014

DSSV++
Δg update of DSSV08

PRL 113, 012001 (2014) PHYSICAL REVIEW LETTERS week ending 4 JULY 2014

Evidence for Polarization of Gluons in the Proton

Daniel de Florian* and Rodolfo Sassot†
Departamento de Física and IFIBA, Facultad de Ciencias Exactas y Naturales, Universidad de Buenos Aires, Ciudad Universitaria, Pabellón 1 (1428) Buenos Aires, Argentina

Marco Stratmann‡
Institute for Theoretical Physics, Tübingen University, Auf der Morgenstelle 14, 72076 Tübingen, Germany and Physics Department, Brookhaven National Laboratory, Upton, New York 11973, USA

Werner Vogelsang§
Institute for Theoretical Physics, Tübingen University, Auf der Morgenstelle 14, 72076 Tübingen, Germany
(Received 17 April 2014; published 2 July 2014)

We discuss the impact of recent high-statistics Relativistic Heavy Ion Collider data on the determination of the gluon polarization in the proton in the context of a global QCD analysis of polarized parton distributions. We find evidence for a nonvanishing polarization of gluons in the region of momentum fraction and at the scales mostly probed by the data. Although information from low momentum fractions is presently lacking, this finding is suggestive of a significant contribution of gluon spin to the proton spin, thereby limiting the amount of orbital angular momentum required to balance the proton spin budget.

DOI: 10.1103/PhysRevLett.113.012001 PACS numbers: 13.88.+e, 12.38.Bx, 13.60.Hb, 13.85.Ni

Introduction.—The gluon helicity distribution function $\Delta g(x)$ of the proton has long been recognized as a fundamental quantity characterizing the inner structure of the nucleon. In particular, its integral $\Delta G \equiv \int_0^1 dx \Delta g(x)$ over all gluon momentum fractions x may in $A^+ = 0$ light-cone gauge be interpreted as the gluon spin contribution to the proton spin [1]. As such, ΔG is a key ingredient to the proton helicity sum rule

$$\frac{1}{2} = \frac{1}{2}\Delta\Sigma + \Delta G + L_q + L_g, \qquad (1)$$

where $\Delta\Sigma$ denotes the combined quark and antiquark spin contribution and $L_{q,g}$ are the quark and gluon orbital angular momentum contributions. For simplicity, we have omitted the renormalization scale Q and scheme dependence of all quantities.

It is well known that the quark and gluon helicity distributions can be probed in high-energy scattering processes with polarized nucleons, allowing access to $\Delta\Sigma$ and ΔG. Experiments on polarized deep inelastic lepton-nucleon scattering (DIS) performed since the late eighties [2] have shown that relatively little of the proton spin is carried by the quark and antiquark spins, with a typical value $\Delta\Sigma \sim 0.25$ [2–4]. The inclusive DIS measurements have, however, very little sensitivity to gluons. Instead, the best probes of Δg are offered by polarized proton-proton collisions available at the BNL Relativistic Heavy Ion Collider (RHIC) [5]. Several processes in pp collisions, in particular jet or hadron production at high transverse momentum p_T, receive substantial contributions from gluon-induced hard scattering, hence, opening a window on Δg when polarized proton beams are used.

The first round of results produced by RHIC until 2008 [5] were combined with data from inclusive and semi-inclusive DIS in a next-to-leading order (NLO) global QCD analysis [3], hereafter referred to as "DSSV analysis". One of the main results of that analysis was that the RHIC data—within their uncertainties at the time—did not show any evidence of a polarization of gluons inside the proton. In fact, the integral of Δg over the region $0.05 \lesssim x \lesssim 0.2$ of momentum fraction primarily accessed by the RHIC experiments was found to be very close to zero. Other recent analyses of nucleon spin structure [4] did not fully include RHIC data; as a result Δg was left largely unconstrained.

Since the analysis [3], the data from RHIC have vastly improved. New results from the 2009 run [6,7] at center-of-mass energy $\sqrt{s} = 200$ GeV have significantly smaller errors across the range of measured p_T. This will naturally put tighter constraints on $\Delta g(x)$ and may extend the range of x over which meaningful constraints can be obtained. A striking feature is that the STAR jet data [6] now exhibit a double-spin asymmetry A_{LL} that is clearly nonvanishing over the whole range $5 \lesssim p_T \lesssim 30$ GeV, in contrast to the previous results. Keeping in mind that, in this regime, jets are primarily produced by gluon-gluon and quark-gluon scattering, this immediately suggests that gluons inside the proton might be polarized. At the same time, new PHENIX data for π^0 production [7] still do not show any significant asymmetry, and it is of course important to reveal whether the two data sets provide compatible information. In this Letter, we assess the impact of the 2009 RHIC data sets on

NNPDFpol1.1
Δg, $\Delta\bar{q}$ update of NNPDFpol1.0

ELSEVIER CrossMark Available online at www.sciencedirect.com ScienceDirect
Nuclear Physics B 887 (2014) 276–308 NUCLEAR PHYSICS B
www.elsevier.com/locate/nuclphysb

A first unbiased global determination of polarized PDFs and their uncertainties

NNPDF Collaboration

Emanuele R. Nocera [b], Richard D. Ball [a], Stefano Forte [b,*], Giovanni Ridolfi [c], Juan Rojo [d,e]

[a] *Higgs Centre, University of Edinburgh, JCMB, KB, Mayfield Rd, Edinburgh EH9 3JZ, Scotland, United Kingdom*
[b] *Dipartimento di Fisica, Università di Milano and INFN, Sezione di Milano, Via Celoria 16, I-20133 Milano, Italy*
[c] *Dipartimento di Fisica, Università di Genova and INFN, Sezione di Genova, Genova, Italy*
[d] *PH Department, TH Unit, CERN, CH-1211 Geneva 23, Switzerland*
[e] *Rudolf Peierls Centre for Theoretical Physics, 1 Keble Road, University of Oxford, OX1 3NP Oxford, United Kingdom*

Received 25 June 2014; received in revised form 17 August 2014; accepted 18 August 2014

Available online 22 August 2014

Editor: Tommy Ohlsson

Abstract

We present a first global determination of spin-dependent parton distribution functions (PDFs) and their uncertainties using the NNPDF methodology: NNPDFpol1.1. Longitudinally polarized deep-inelastic scattering data, already used for the previous NNPDFpol1.0 PDF set, are supplemented with the most recent polarized hadron collider data for inclusive jet and W boson production from the STAR and PHENIX experiments at RHIC, and with open-charm production data from the COMPASS experiment, thereby allowing for a separate determination of the polarized quark and antiquark PDFs, and an improved determination of the medium- and large-x polarized gluon PDF. We study the phenomenological implications of the NNPDFpol1.1 set, and we provide predictions for the longitudinal double-spin asymmetry for semi-inclusive pion production at RHIC.

* Corresponding author.

http://dx.doi.org/10.1016/j.nuclphysb.2014.08.008

Impact of data: W production in pp collisions

Observable

$$A_L = \frac{\sigma^+ - \sigma^-}{\sigma^+ + \sigma^-}$$

Features

- at RHIC, $\langle x_{1,2} \rangle \simeq \frac{M_W}{\sqrt{s}} e^{-\eta_l/2} \approx [0.04, 0.4]$
- A_L sensitive to Δq, $\Delta \bar{q}$ at $Q \sim M_W$ (no need of fragmentation functions)

$$A_L^{W^-} \sim \frac{\Delta \bar{u}_{x_1} d_{x_2} (1 - \cos\theta)^2 - \Delta d_{x_1} \bar{u}_{x_2} (1 + \cos\theta)^2}{\bar{u}_{x_1} d_{x_2} (1 - \cos\theta)^2 - d_{x_1} \bar{u}_{x_2} (1 + \cos\theta)^2}$$

backward lepton rapidity forward lepton rapidity

- for W^+, $d \longleftrightarrow u$ and $\Delta d \longleftrightarrow \Delta u$
- no access to strangeness ($W^\pm$ + c)

Measurements

- STAR [PRL 113 (2014) 072301]
- PHENIX [PRD 93 (2016) 051103]

Effects

First evidence of broken flavor symmetry for polarised light sea quarks

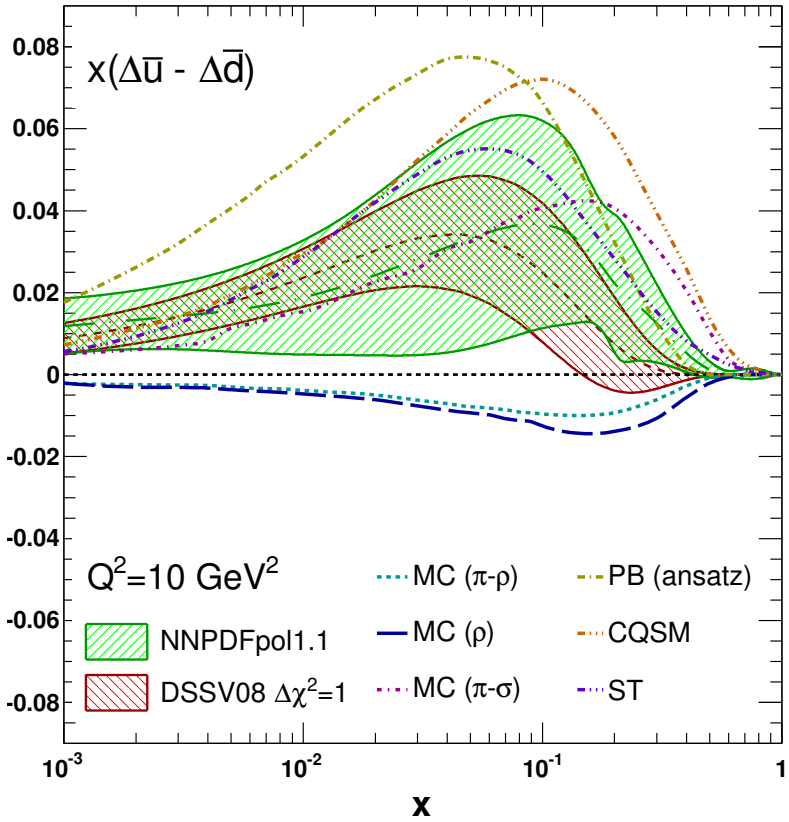

- $\Delta \bar{u} > 0 > \Delta \bar{d}$, $|\Delta \bar{d}| > |\Delta \bar{u}|$
- $|\Delta \bar{u} - \Delta \bar{d}| \sim |\bar{u} - \bar{d}|$
- some models are disfavored

Impact of data: jet and π production

Observable

$$A_{LL} = \frac{\sigma^{++} - \sigma^{+-}}{\sigma^{++} + \sigma^{+-}}$$

Features

- at RHIC,
  $\langle x_{1,2} \rangle \simeq \frac{2p_T}{\sqrt{s}} e^{-\eta/2} \approx [0.05, 0.2]$
- qg,gg initiated subprocesses dominate (for most of the RHIC kinematics)
- A_{LL} sensitive to Δg

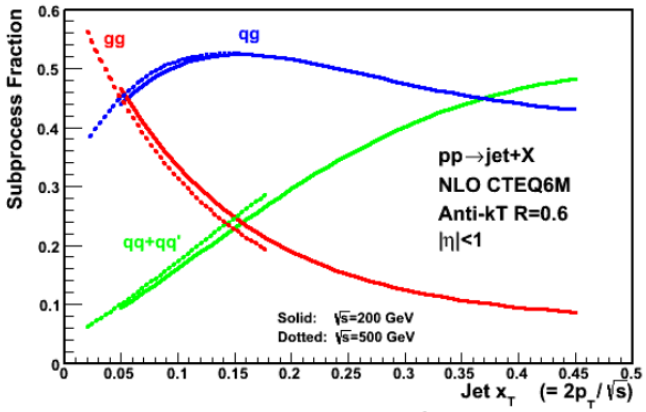

Measurements

- STAR (jets) [PRL 115 (2015) 092002]
- PHENIX (π) [PRD 90 (2014) 012007]

Effects

First evidence of a sizable, positive gluon polarization in the proton

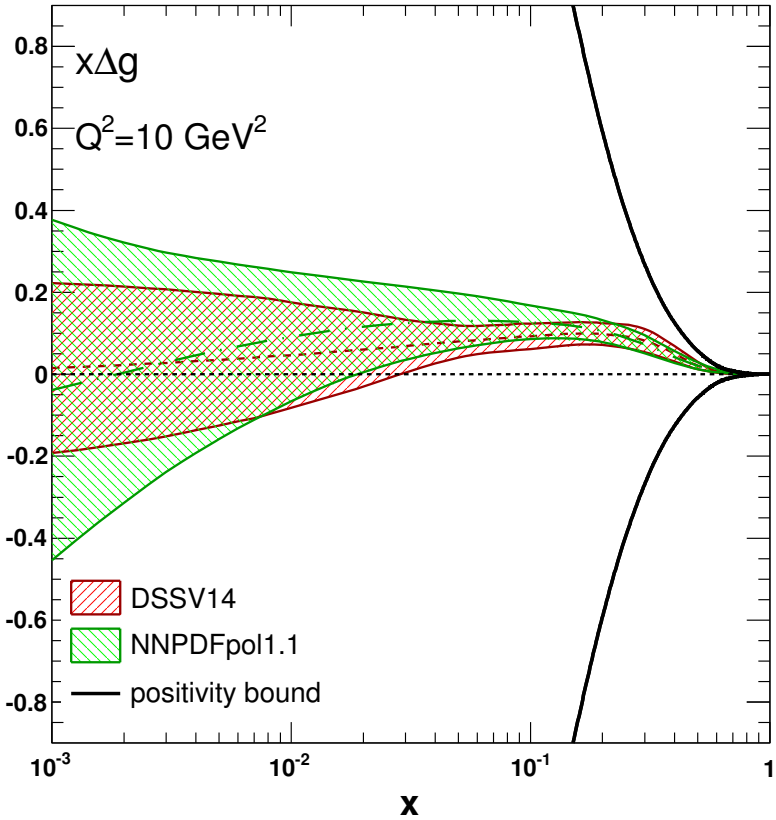

$Q^2 = 10$ GeV^2	$\int_{0.05}^{0.2} dx \Delta g(x, Q^2)$
NNPDFpol1.1	$+0.15 \pm 0.06$
DSSV14	$0.10^{+0.06}_{-0.07}$

Open issues: the spin content of the proton

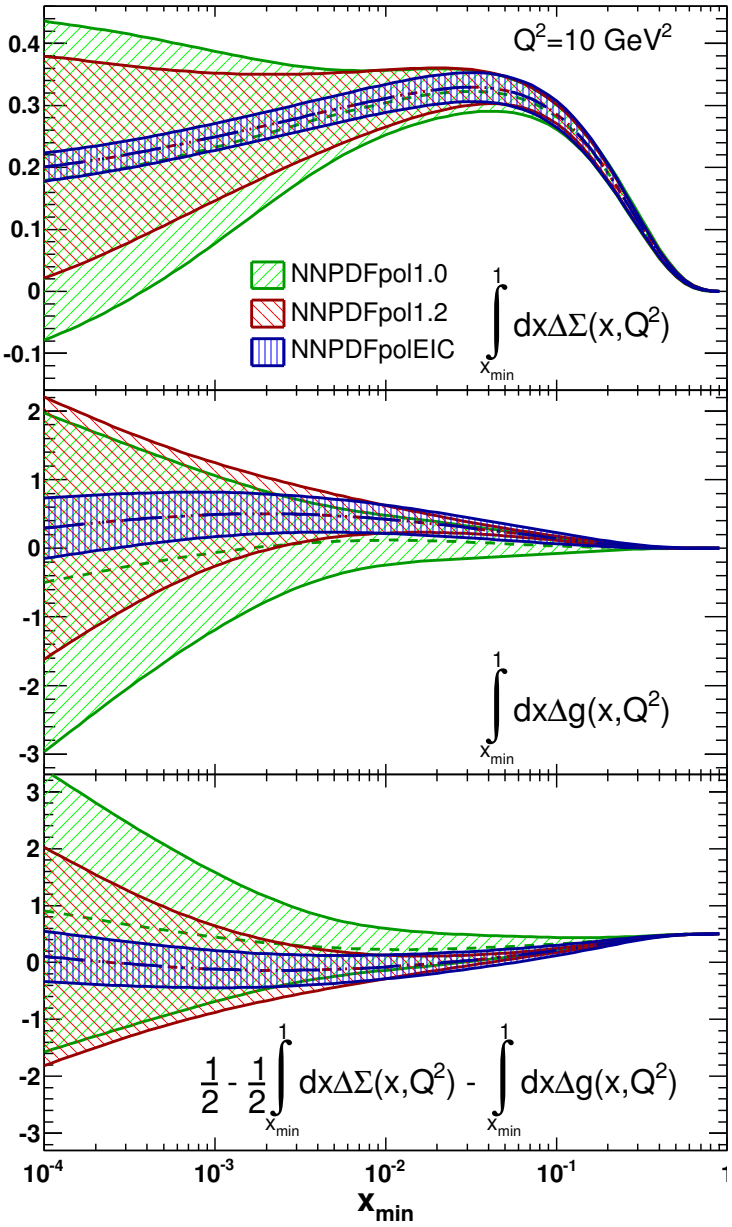

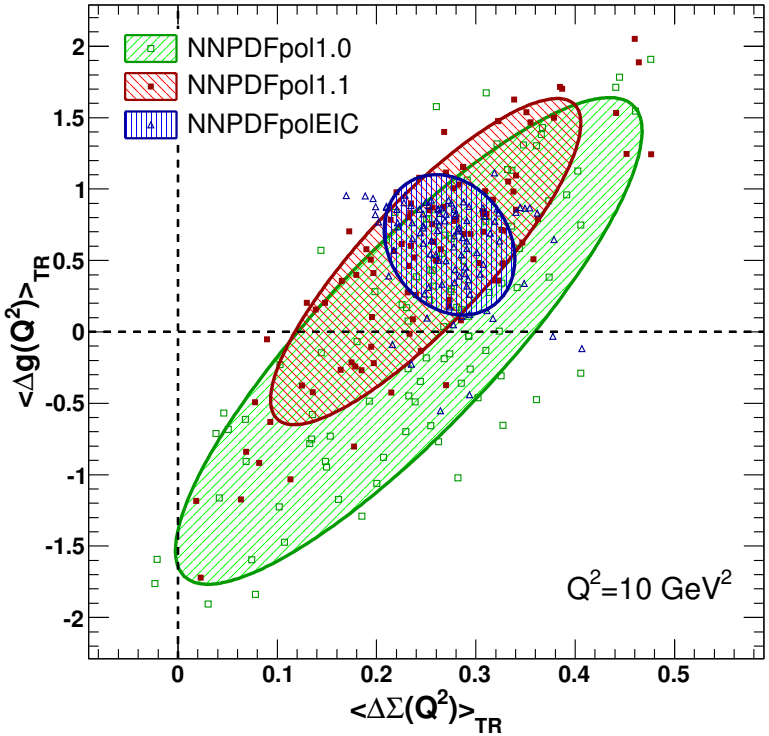

$Q^2 = 10$ GeV^2	$\int_{10^{-3}}^{1} dx\ \Delta\Sigma$	$\int_{10^{-3}}^{1} dx\ \Delta g$
NNPDFpol1.0	$+0.23 \pm 0.15$	-0.06 ± 1.12
NNPDFpol1.2	$+0.25 \pm 0.10$	$+0.49 \pm 0.75$
NNPDFpolEIC	$+0.24 \pm 0.04$	$+0.49 \pm 0.25$

quarks and antiquarks $\sim 20\% - 30\%$
gluons $\sim 70\%$
OAM $\sim 0\%$

Open issues: SU(3) breaking and strangeness

NNPDFpol1.0 [NPB 874 (2013) 36]
$\int_0^1 dx[\Delta s + \Delta\bar{s}] = -0.13 \pm 0.09$

Lattice [PRL 108 (2012) 222001]
$\int_0^1 dx[\Delta s + \Delta\bar{s}] = -0.020(10)(1)$

First moment constrained by
$a_3 = \int_0^1 dx[\Delta u^+ - \Delta d^+]$
$= 1.2701 \pm 0.0025$

$a_8 = \int_0^1 dx[\Delta u^+ + \Delta d^+ - 2\Delta s^+]$
$= 0.585 \pm 0.025$

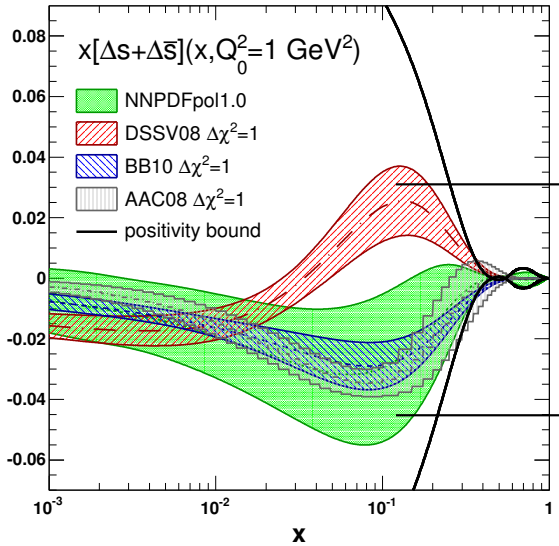

directly from SIDIS Kaon data

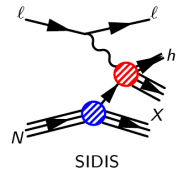

indirectly from DIS + SU(3)

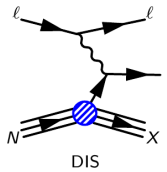

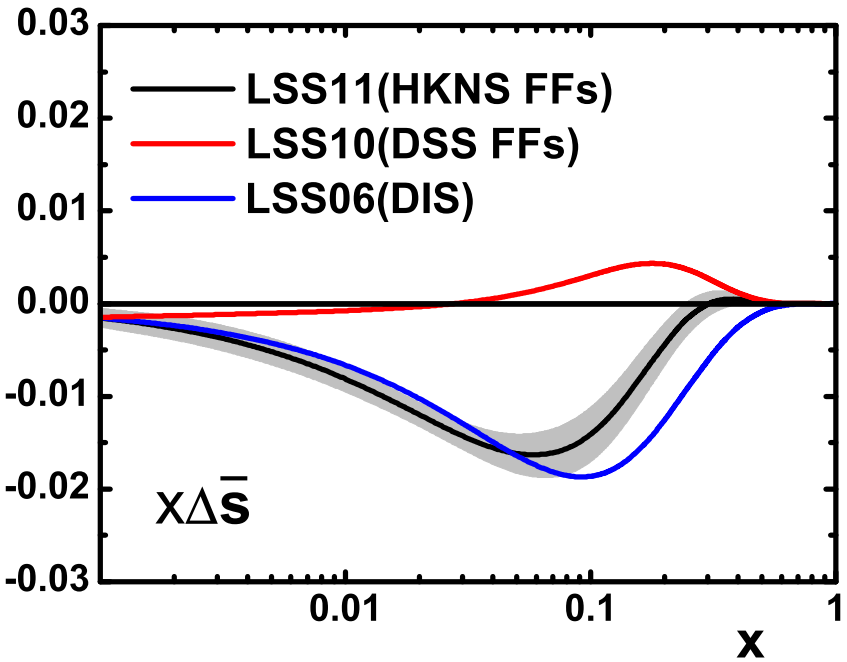

Open issues: SU(3) breaking and strangeness

NNPDFpol1.0 [NPB 874 (2013) 36]
$\int_0^1 dx[\Delta s + \Delta\bar{s}] = -0.13 \pm 0.09$

Lattice [PRL 108 (2012) 222001]
$\int_0^1 dx[\Delta s + \Delta\bar{s}] = -0.020(10)(1)$

First moment constrained by
$a_3 = \int_0^1 dx[\Delta u^+ - \Delta d^+]$
$= 1.2701 \pm 0.0025$

$a_8 = \int_0^1 dx[\Delta u^+ + \Delta d^+ - 2\Delta s^+]$
$= 0.585 \pm 0.025$

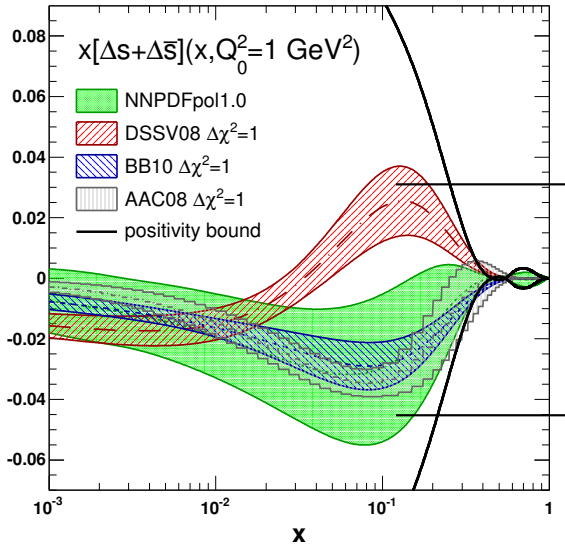

directly from SIDIS Kaon data

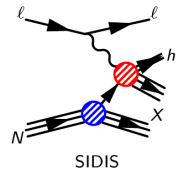

indirectly from DIS + SU(3)

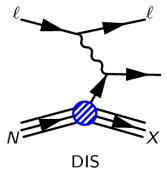

All PDF determinations based only on DIS data (+ SU(3)) find a negative Δs^+
PDF determinations based on DIS+SIDS data (+SU(3)) find a negative or a postive Δs^+ depending on the K FF set

Is there mounting tension between DIS and SIDIS data?

$SU(3)$ may be broken [PRD 58 (1998) 094028, Ann.Rev.Nucl.Part.Sci. 53 (2003) 39], but how much?
$\longrightarrow$ in `NNPDFpol1`, the nominal uncertainty on a_8 in inflated by 30% of its value to allow for a $SU(3)$ symmetry violation ($a_8 = 0.585 \pm 0.025 \longrightarrow a_8 = 0.585 \pm 0.176$)
$\longrightarrow$ but *e.g.* lattice finds a larger $SU(3)$ symmetry violation [PRL 108 (2012) 222001]

No neutrino DIS data so far

Inclusion of SIDIS data requires the knowledge of the fragmentation $s \to K$
$\longrightarrow$ how well do we know the kaon fragmentation function?

3.5 A simultaneous determination of PDFs/FFs

The idea [arXiv:1705.05889]

1. Perform a simultaneous determination of polarised PDFs and FFs
   from all available data of polarised DIS, polarised SIDIS and SIA

$$d\sigma^{\rm DIS} = \sum_f d\hat{\sigma}^{\rm DIS} \otimes \Delta f$$

$$d\sigma^{\rm SIDIS} = \sum_f d\hat{\sigma}^{\rm SIDIS} \otimes \Delta f \otimes D_f$$

$$d\sigma^{\rm SIA} = \sum_f d\hat{\sigma}^{\rm SIA} \otimes D_f$$

2. Release usual SU(2) and SU(3) constraints used in all other analyses

$$\int_0^1 dx(\Delta u^+ - \Delta d^+) \stackrel{?}{=} g_a$$

$$\int_0^1 dx(\Delta u^+ + \Delta d^+ - s\Delta s^+) \stackrel{?}{=} a_8$$

3. Use the Iterative Monte Carlo fitting procedure
   statistically sound representation of experimental uncertainties
   avoid potential biases introduced by fixing parameters not well constrained by the data

Recap of the Iterative Monte Carlo procedure

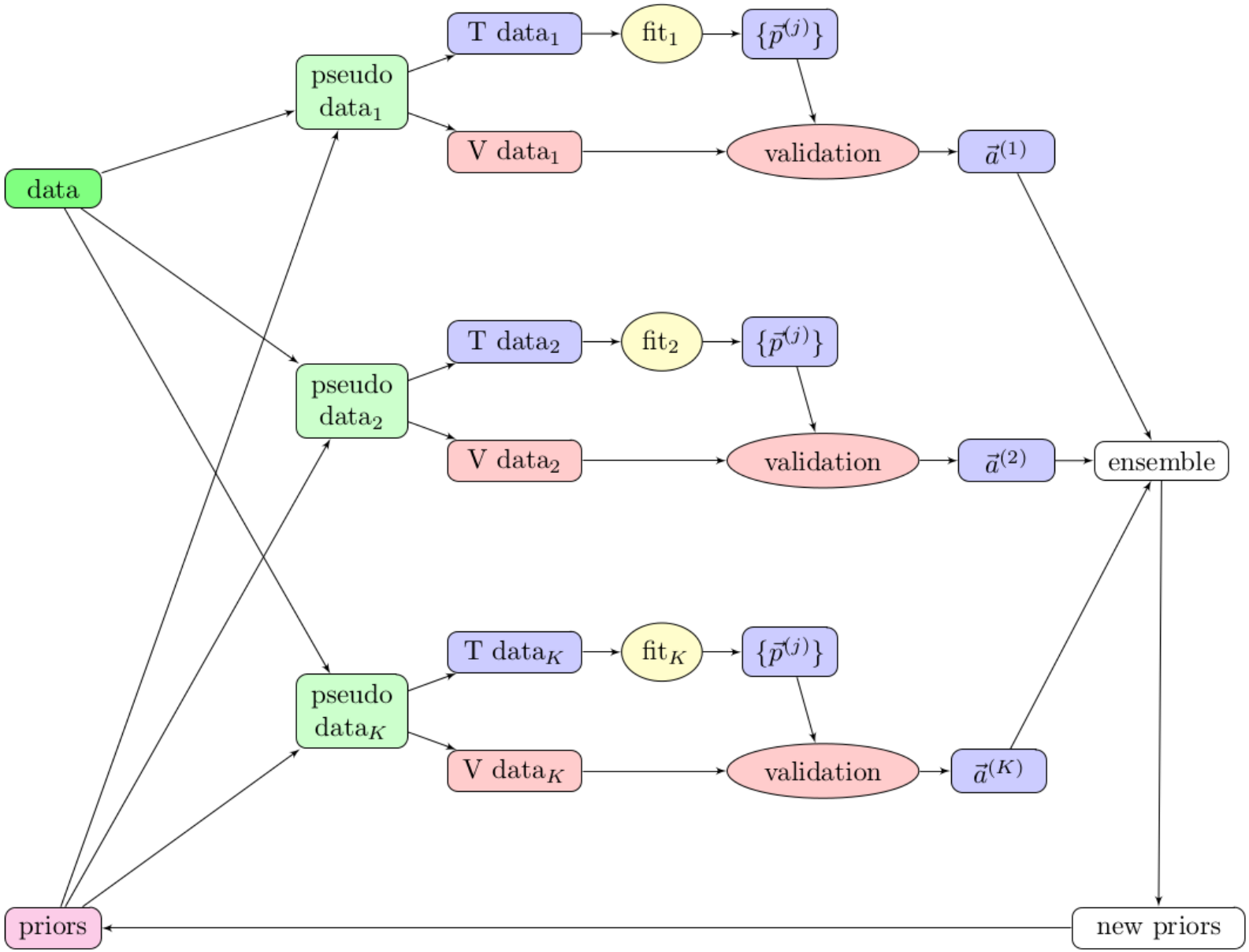

Fit settings

Physical parameters: as in previous JAM analyses [PRD 93 (2016) 074005; PRD 94 (2016) 114004]

$$\alpha_s(M_Z) = 0.118,\ \alpha(M_Z) = 1/127,\ m_c = 1.43 \text{ GeV},\ m_b = 4.3 \text{ GeV}$$

Solution of DGLAP equations: numerical solution in N-space

Parametrisation: template functional form at $Q_0 = 1$ GeV

$$T(x, \{a\}) = \frac{M x^a (1-x)^b (1 + c\sqrt{x})}{B(n+a, 1+b) + cB(n+1/2+1, 1+b)}$$

PDFs: $n = 1$ Δq^+, $\Delta \bar{q}$, $\Delta g = T(x, \{a\})$ FFs: $n = 2$, $c = 0$

PIONS

$$D_{\bar{u}}^{\pi^+} = D_d^{\pi^+} = T(z, \{a\})$$
$$D_s^{\pi^+} = D_{\bar{s}}^{\pi^+} = \tfrac{1}{2} D_{s+}^{\pi^+}$$

KAONS

$$D_{\bar{u}}^{K^+} = D_d^{K^+} = \tfrac{1}{2} D_{d+}^{K^+}$$
$$D_s^{K^+} = T(z, \{a\})$$

assume charge conjugation, from which $D_{q^+}^{\pi^+} = D_{q^+}^{\pi^-}$

Heavy flavours: heavy-quark FFs are parametrised independently at their thresholds

Kinematic cuts: remove small-z SIA data and large-x, small-Q^2 (SI)DIS data

PIONS

$z_{\min} = 0.1$, $z_{\min} = 0.05$ ($\sqrt{s} = M_Z$)

$Q_0^2 > 1$ GeV, $W^2 > 10$ GeV^2

KAONS

$z_{\min} = 0.2$ ($\sqrt{s} = 10$ GeV), $z_{\min} = 0.1$

$Q_0^2 > 1$ GeV, $W^2 > 10$ GeV^2

Fit quality and strangeness

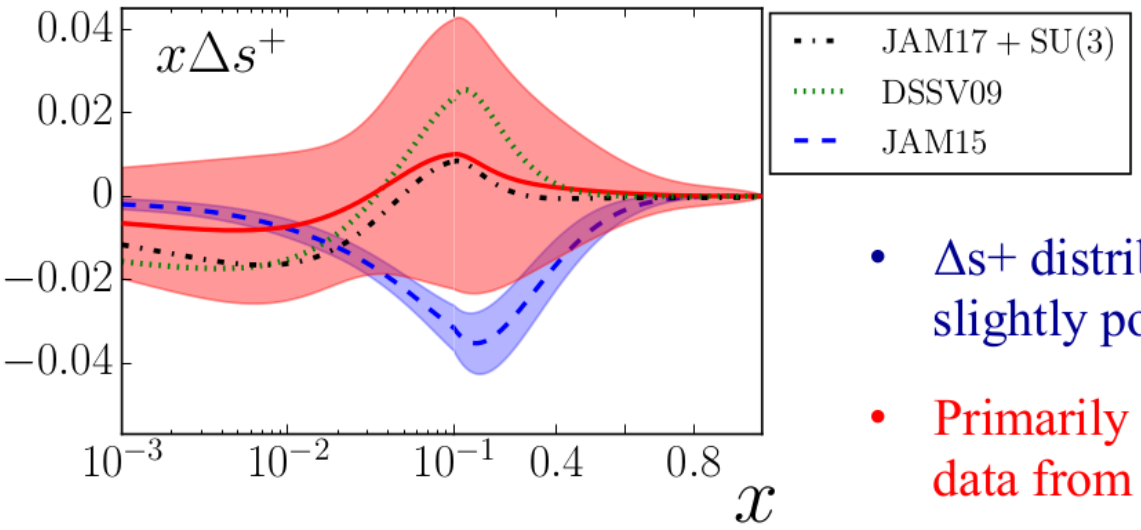

process	target	$N_{\rm dat}$	χ^2
DIS	$p, d, {}^3$He	854	854.8
SIA $(\pi^\pm, K^\pm)$		850	997.1
SIDIS $(\pi^\pm)$			
HERMES	d	18	28.1
HERMES	p	18	14.2
COMPASS	d	20	8.0
COMPASS	p	24	18.2
SIDIS $(K^\pm)$			
HERMES	d	27	18.3
COMPASS	d	20	18.7
COMPASS	p	24	12.3
Total:		**1855**	**1969.7**

- Δs+ distribution consistent with zero, slightly positive in intermediate x range
- Primarily influenced by HERMES K-data from deuterium target

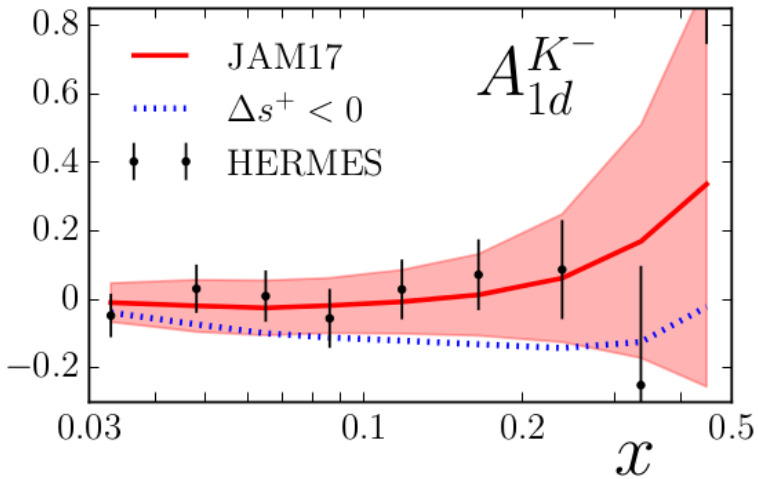

Slide: courtesy of J. Ethier

Moments

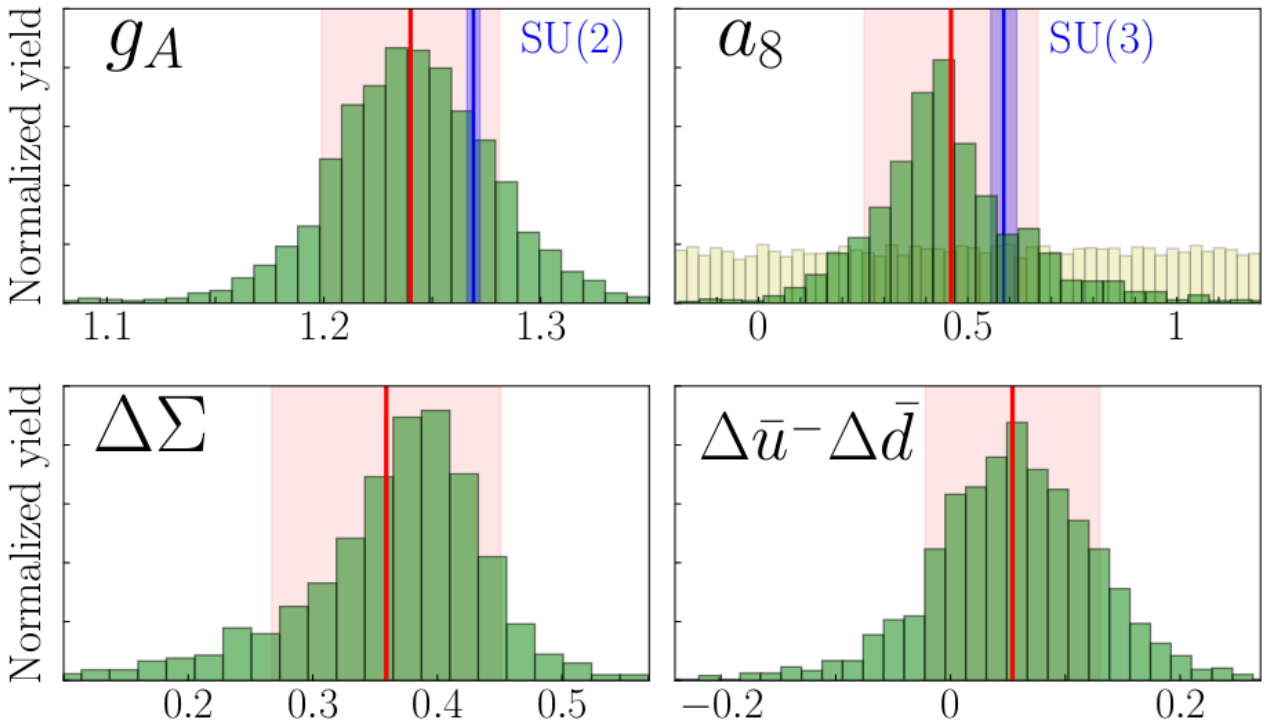

$$g_A = 1.24 \pm 0.04$$ Confirmation of SU(2) symmetry to ~2%

$$a_8 = 0.46 \pm 0.21$$ ~20% SU(3) breaking ± ~20%; large uncertainty

- Need better determination of Δs+ moment to reduce a_8 uncertainty!

$$\Delta \mathbf{s}^+ = -0.03 \pm 0.09$$

Slide: courtesy of J. Ethier

Moments

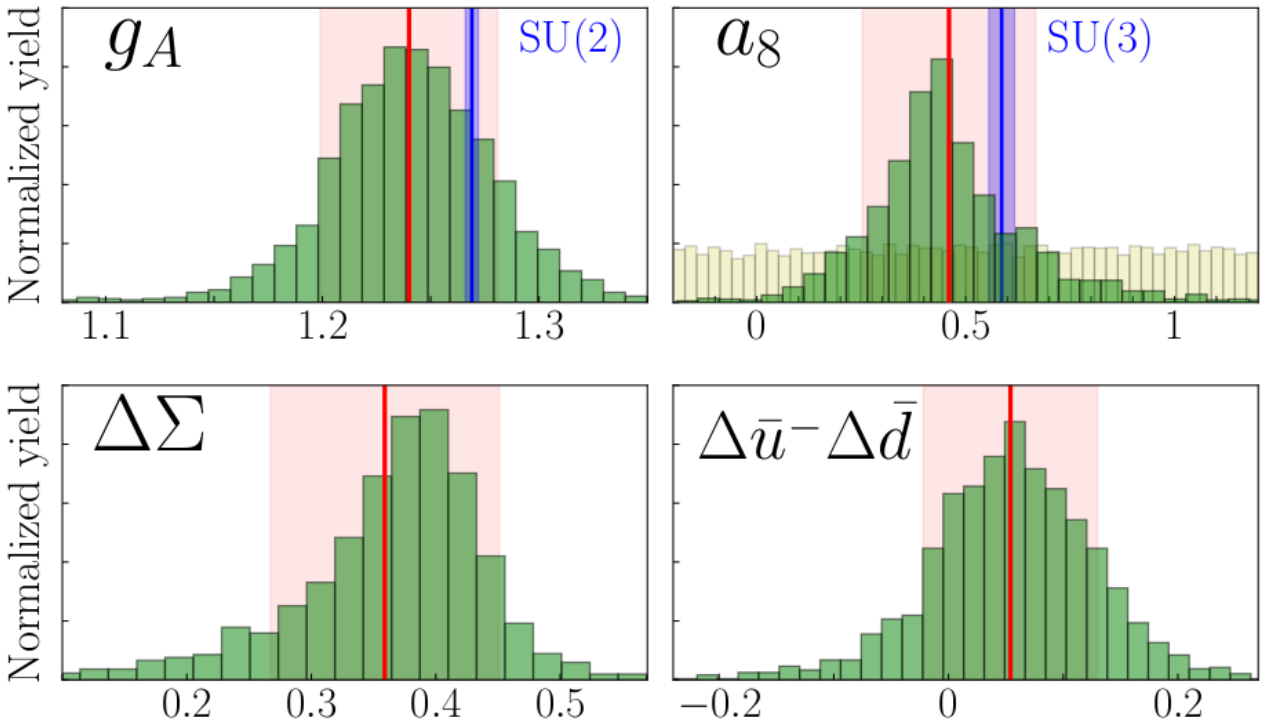

$$\Delta\Sigma = 0.36 \pm 0.09$$

Slightly larger central value than previous analyses, but consistent within uncertainty

Preference for slightly positive sea asymmetry; not very well constrained by SIDIS

$$\Delta\bar{u} - \Delta\bar{d} = 0.05 \pm 0.08$$

Slide: courtesy of J. Ethier

3.6 Summary of Lecture 3

Summary

1. Fits to SIA data only
   - $\longrightarrow$ overall good description of the data
   - $\longrightarrow$ theoretical improvements consistently result in fit improvements
   - $\longrightarrow$ residual signs of tensions among some experiments in some kinematic regions
2. Global fits
   - $\longrightarrow$ overall good description of the global data set
   - $\longrightarrow$ stress-test for FF universality/QCD factorisation
3. The spin structure of the proton
   - $\longrightarrow$ SIDIS provides an importannt piece of experimental information
   - $\longrightarrow$ SIDIS might bias a determination of polarised PDFs
4. The first simultaneous determination of polarised PDFs and FFs
   - $\longrightarrow$ properly assess cross-talks among various nonperturbative distributions
   - $\longrightarrow$ possible solution of the strangeness conundrum

Ultimate goal
a simultaneous global determination of unpolarised/polarised PDFs and FFs

End of my lectures
Thank you very much for your attention